INVESTIGATING DIGIT LOSS IN *STRUTHIO CAMELUS*

By
Rushil Lala

A dissertation submitted to the Faculty of Science, University of the Witwatersrand, Johannesburg, in fulfilment of the requirements for the degree of Master of Science

Johannesburg, August 2017

Declaration

I, Rushil Lala (437460) , am a student registered for the degree of MSc (Dissertation) in the academic year 2017.
I hereby declare the following:

- I am aware that plagiarism (the use of someone else's work without their permission and/or without acknowledging the original source) is wrong.
- I confirm that the work submitted for assessment for the above degree is my own unaided work except where explicitly indicated otherwise and acknowledged.
- I have not submitted this work before for any other degree or examination at this or any other University.
- The information used in the Dissertation Report **HAS NOT** been obtained by me while employed by, or working under the aegis of, any person or organisation other than the University.
- I have followed the required conventions in referencing the thoughts and ideas of others.
- I understand that the University of the Witwatersrand may take disciplinary action against me if there is a belief that this is not my own unaided work or that I have failed to acknowledge the source of the ideas or words in my writing.

signature 

31st day of July 2017

Abstract

Vertebrate limb development is controlled by an elaborate and complex network of developmental genes and pathways. Alterations in the expression of these genes has resulted in the evolution of a diverse range of limb morphologies adapted to environmental and functional needs. One particular vertebrate with a unique limb morphology is the ostrich (*Struthio camelus*). *S. camelus* possesses two digits on its hind limb making the limb lighter and more better adapted to running on plains. It has been observed during the development of *S. camelus* that five digit primordia arise in early development, only for three to be eliminated later in the development process. We hypothesised that these digits are lost during a post pattering process involving programmed cell death driven by the genes *Msx2* and *Bmp4*. In this investigation we utilise whole mount *in situ* hybridisation to show that *Msx1* and *Msx2* expression expands into the domains of the eradicated digits. TUNEL assays and immunocytochemistry using Sox9 antibodies show a reduction in digit primordia, and possible co-localisation of apoptotic nuclei with the eradicated digits. The recapitulation of the *S. camelus Msx2* promoter expression in *G. gallus* was not achieved, but it is shown that a 3.5kb upstream region of *S. camelus Msx2* gene is able to drive expression in *G. gallus*. Despite this, presented data is sufficient to suggest that digit loss in the developing hind limb of *S. camelus* takes place post patterning and is driven by *Msx1* and *Msx2* programmed cell death pathways.

Acknowledgments

I would like to acknowledge and thank the following:

- My supervisor Dr N. Nikitina
- National Research Foundation
- Prof U. Ripamonti and Mrs R. Parak of the Bone Research Unit
- Mr P. Selahle of the Central Animal Services
- The Agricultural Research Council
- Buffelskom Boerdery

Table of Content

Abstract 3

Acknowledgments 4

I. List of Figures 7

II. List of Table 8

III. List of Appendices 8

1.1 Tetrapod Limb Development 9

1.2 Limb Modification 14

1.4 Programmed Cell Death During Limb Development 18

1.5 Apoptotic Genes 22

1.5.1 Bmp4 22

1.5.2 Msx1 and Msx2 23

2.1 Tissue Dissection 25

2.2 Nucleic Acid Extraction 26

2.3 Whole Mount In Situ Hybridisation 26

2.3.1 RT-PCR 26

2.3.2 PCR 27

2.3.3 Cloning 27

2.3.4 Probe Synthesis 28

2.3.5 Whole-mount In Situ Hybridisation 29

2.4 Cell Death Assay 31

2.4.1 Cryosectioning 31

2.4.2 TUNEL and Immunocytochemistry 32

2.5 Msx2 Promoter Analysis 33

2.5.1 Bioinformatics 33

2.5.2 PCR 33

2.5.3 Cloning 34

2.5.4 Electroporation 35

3. Results 37

3.1 Nucleic Acid Extraction 37

3.2 G. gallus Bmp4 Cloning 37

3.2 Probe Synthesis 40

3.3.1 Bmp expression 42

3.3.2 Msx Expression 43

3.3.3 Expression of Additional Genes 45
3.4 TUNEL and Immunocytochemistry 46
3.5 Promoter Analysis 47
4.1 Msx expression patterns in S. camelus suggests its possible role in elimination digit primordia 49
4.2 Loss of digit primordia in S. camelus could be as a result of apoptosis 50
4.3 Bmp expression in G. gallus interdigital regions points to a role in PCD 50
4.4 Expression of Shh, Sox9 and Fgf10 could have rules out other mechanisms of digit loss 51
4.5 S. camelus Msx2 promoter is able to drive expression in G. gallus 52
4.6 Conclusion 53
4.7 Further work 54
5.1 Appendix A 55
5.2 Appendix B 56
6. References 57

I. List of Figures

Figure 1 - A graphical guide to the limb axes

Figure 2 - Diagram of the expression patterns of various developmental genes

Figure 3 - Structures of the modified pentadactyl limbs of the aye-aye, bat and duck.

Figure 4 – Structure of the oligodactyl limbs of the two-toed earless skink and the cow

Figure 5A - Phylogenetic tree of oligodactyl vertebrates

Figure 5B- Limbs of the oligodactylous vertebrates

Figure 6 - Nucleic acid extraction of *G. gallus* and *S. camelus* gDNA and *G. gallus* RNA

Figure 7 - cDNA synthesis from *G. gallus* RNA and *Bmp4* PCR

Figure 8 - Linearisation of *Bmp2, Bmp4, Fgf10* and *Shh* containing plasmids

Figure 9 - Synthesis of *Bmp2, Bmp4, Fgf10* and *Shh* probes

Figure 10 - WISH on *G. gallus* limbs with *G. gallus Bmp* RNA probes

Figure 11 - WISH on *G. gallus* and *S. camelus* limbs with *G. gallus Msx1* RNA probes

Figure 12 - WISH on *G. gallus* and *S. camelus* limbs with *G. gallus Msx2* RNA probes

Figure 13 - WISH on *G. gallus* limbs with *Fgf10, Sox9* and *Shh* probes of *G. gallus*

Figure 14 - TUNEL assay and ICC on *S. camelus* limb sections

Figure 15 - *S. camelus Msx2* promoter region PCR

Figure 16 - Fluorescent expression in *G. gallus* embryonic tissue after electroporation

II. List of Table

Table 1- Enzymes used for plasmid linearisation and RNA probe transcription

Table 2- Conditions of *S. camelus Msx2* promoter region PCR

III. List of Appendices

Appendix A- Whole mount i*n situ* hybridisation reagents

Appendix B- Figure 5B image sources

Introduction

1.1 Tetrapod Limb Development

The development of specialised tetrapod limbs is a complex process orchestrated by numerous developmental genes during embryogenesis. Distinct spatial and temporal gene expression patterns drive tissues to develop and regress, resulting in a variety of different limb morphologies.

Tetrapod limbs develop along three axes (Figure 1): the proximal to distal axis (PD axis), which runs from the body to the digit tips, the dorsal to ventral axis (DV axis), which goes from the back of the hand to the palm, and the anterior to posterior axis (AP axis) which starts at digit I (thumb) and extends to digit V (the little finger).

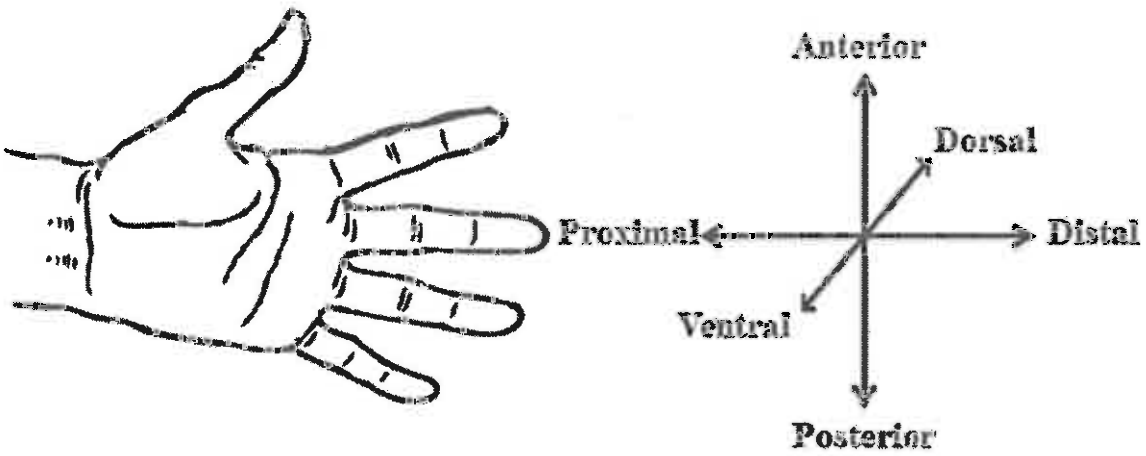

Figure 1 Graphical guide to the limb axes. The proximal-distal axis of the limb runs from the shoulder or pelvis to the tips of the digits. The dorsal-ventral axis runs from the top of the limb to the bottom of the limb, that is the palm of the hand or sole of the foot. The anterior-posterior axis runs from digit I to digit number V, or thumb to little finger.

The PD axis is established through the action of the apical ectodermal ridge (AER) (Figure 2A). The AER is a localised region of ectodermal tissue situated at the apex of the developing limb bud, which maintains the growth and undifferentiated state of the limb bud mesenchyme by secreting fibroblast growth factors (Fgfs) (Sun, Mariani and Martin, 2002). The role of the AER in limb development is apparent by the fact that the excision of the AER leads to incomplete and stunted growth of limbs (Saunders, 1948; Summerbell, 1974; Rowe and Fallon, 1982). The AER is initiated when *Wnt3a* expression is activated in the lateral plate mesoderm by *Fgf10*, which in turn activates *Fgf8* (Kawakami *et al.*, 2001; Logan, 2003). The T-box genes, *Tbx5* in the forelimb and *Tbx4* in the hind limb, also play a role in limb bud outgrowth and initiation. It is observed that zebrafish with *Tbx5* knockout fail to develop pectoral fins (Rodriguez-Esteban *et al.*, 1999; Ahn *et al.*, 2002). Fgf8 then upregulates *Fgf10* expression in the mesenchyme, establishing a positive feedback loop (Moon and Capecchi, 2000). *Fgf10* is essential for limb bud outgrowth as evidenced by the observation that mice deficient of *Fgf10* are born without hind- or forelimbs (Sekine *et al.*, 1999). Additionally, the application of beads soaked in Fgf1, Fgf2 or Fgf4 can induce the ectopic growth of limbs, indicating functional redundancy (Cohn *et al.*, 1995). It is these *Fgf* signals which result in the elongation of the limb bud and establish the PD axis, Although *Fgf8* is the predominant *Fgf* in the formation of the PD axis. Ectopic application of Fgf8 to the chick flank is able to induce additional limbs while Fgf8 alone can functionally replace the excised AER and maintain *Shh* expression (Vogel, Rodriguez and Izpisúa-Belmonte, 1996).

A second major signalling centre located in the developing limb bud is the zone of polarising activity (ZPA)(Figure 2A, 2B and 2C), a region of mesenchymal tissue located at the posterior region of the developing limb bud (Wolpert, 1969; Fallon and Crosby, 1977). The main signalling molecule expressed from the ZPA, sonic hedgehog (Shh), diffuses across the limb bud creating a Shh gradient (Riddle *et al.*, 1993). The grafting of ZPA tissue or the application

of exogenous Shh to the anterior chick limb buds results in a limb with a mirrored symmetry about the second digit, having the digit pattern: IV, III, II, II, III, IV (Tickle, Summerbell and Wolpert, 1975; Riddle *et al.*, 1993). However, the establishment of the AP axis in the limb bud takes place before Shh expression. *Hand2*, *Gli3,* and several *Hox* genes are upstream regulators of *Shh*. Prior to *Shh* expression, *Hand2* is expressed in the posterior region of the limb bud. Mice with *Hand2* deletions display no *Shh* upregulation, while ectopic expression of *Hand2* is accompanied by ectopic *Shh* expression (Charité, McFadden and Olson, 2000). *Hand2* expression is restricted to the limb posterior by Gli3, while Hand2 restricts *Gli3* expression to the anterior of the limb bud (Te Welscher *et al.*, 2002). Gli3 (Figure 2C) is also a downstream regulator of *Shh* which occurs in two isoforms: The *Shh* repressor Gli3R and the *Shh* activator Gli3A. Gli3R is a truncated isoform occurring in higher concentrations at the anterior of the limb bud where the Shh concentration is lower. Gli3A is a full length isoform found in higher concentrations on the posterior limb bud where the Shh concentration is higher (Litingtung *et al.*, 2002). This is due to the fact that Shh prevents the proteolytic truncation of Gli3A (Wang, Fallon and Beachy, 2000). The antagonistic roles of these two genes are made apparent by the fact that $Gli3^{-/-}$ null mutants display polydactyly, whereas $Shh^{-/-}$ null mutants display syndactyly (Litingtung *et al.*, 2002; te Welscher *et al.*, 2002). *Shh* also acts in a feedback loop with *Fgf4, -9* and *-17* to maintain the AER by upregulating the Bmp antagonist, *Gremlin,* which prevents *Bmp's* from down regulating the *fgfs* (Capdevila *et al.*, 1999; Pizette and Niswander, 1999; Zúñiga *et al.*, 1999; Sun *et al.*, 2000).

Shh signalling is also regulated by Ptch1 and Ptch2. Ptch proteins are transmembrane proteins which sequester Shh to restrict its distribution and establish a gradient (Chen and Struhl, 1996). Ptch1 and 2 are Shh receptors which transduce Shh signalling when bound to Shh and inhibit the signalling pathway when unbound (Chen and Struhl, 1996; Briscoe *et al.*, 2001). One of

the pathways activated is that which leads to the expression of *Gli3*. (Varjosalo and Taipale, 2007)

Another set of genes involved in AP polarity are *Hox* genes, particularly *HoxA* and *HoxD* genes. 5' *HoxA* genes are required to initiate *Shh* expression in the ZPA, Shh then maintains the expression of *HoxD* genes in the limb bud (Kmita *et al.*, 2005). *Hoxd9* is expressed throughout the entire limb bud, *Hoxd10-11* are expressed in the posterior two thirds of the bud, and *Hoxd12-13* are expressed in the posterior third of the limb bud (Tickle, 2006) (Figure 2D). These *HoxD* genes play a regulatory role in the patterning process such as the positive regulation of limb out growth and PD axis specification. This is apparent when looking at the phenotypes of mice with individual *HoxD* genes knocked out, which display shortened and fused digits, the lack of digit I, malformed wrist bones and shortened, or sometimes completely lacking, forearm bones (Dolle *et al.*, 1993; Favier *et al.*, 1996; Fromental-Ramain *et al.*, 1996). Other evidence suggests that *HoxD* genes also negatively regulate digit number as seen from the fact that mice with knockout *Gli3*($Gli3^{Xtl/Xtl}$) and *Hoxd 11-13*($Hoxd^{Del(11-13)/(11-13)}$) are severely polydactylous with as many as eleven digits on the forlimb (Sheth, Bastida and Ros, 2007).

The truncation of distal limb structures also indicates that *Hox* genes play a role in PD axis development, particularly AER formation. *Hox* paralogs 8-11 are primarily involved in AER initiation and maintenance (Tarchini, Duboule and Kmita, 2006; Zakany, Zacchetti and Duboule, 2007).

The dorso-ventral axis is established by four genes: Radical fringe (*r-Fng*), *Wnt-7a* and LIM-homeodomain (*Lmx-1*) which are expressed dorsally, and Engrailed-1 (*En-1*) which is expressed ventrally (Dealy *et al.*, 1993; Riddle *et al.*, 1995). The ventrally expressed EN-1, restricts the expression of *r-Fng* and *Wnt-7a* to the dorsal portion of the limb (Davis and Joyner,

1988). WNT-7a initiates the expression of *Lmx-1* which is the main DV axis determination factor (Vogel *et al.*, 1995) (Figure 2E). The border between *En-1* and *r-Fng* expression is where the AER is formed (Laufer *et al.*, 1997).

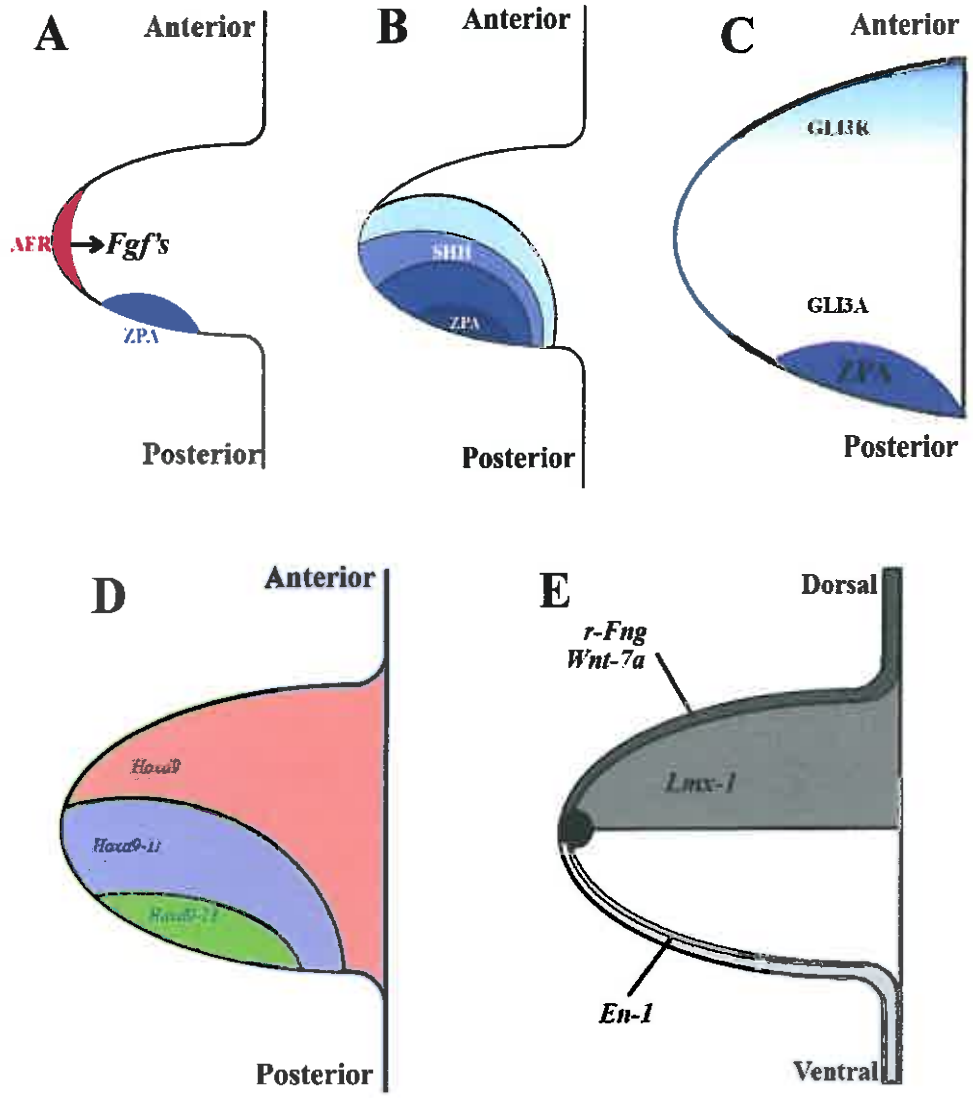

Figure 2 The various signalling molecules responsible for vertebrate limb patterning. 2A) The two main signalling centres: the AER (red) which secretes various Fgfs, and the ZPA (blue) responsible for Shh secretion. 2B)The Shh gradient originating from the ZPA. 2C)The gradient and distribution of GLI3A (white) and GLI3R (light blue) in relation to the ZPA. 2D)The distribution of *Hox* genes throughout the developing limb bud. 2E) shows the genes involved in DV specification. r-Fng and Wnt-7a in the dorsal epithelium, Lmx-1 in the dorsal mesenchyme and En-1 in the ventral epithelium. The black dot at the apex is where the AER forms.

1.2 Limb Modification

Through alterations in the expression of the above mentioned genes, tetrapod limbs have become modified for more efficient locomotion or specialised functions such as flight. In most cases the molecular mechanisms responsible for these modifications are unclear due to the difficulties related to work on atypical model organisms. The most common of limb modification is digit loss, where tetrapods may possess fewer digits per limb than the pentadactyl (five-digit) ground state. These morphological changes evolved for more efficient locomotion because a limb with fewer digits is lighter and expends less energy during movement, additionally a limb with fewer digits has a smaller surface area which makes navigating uneven terrains easier (Lande, 1978; Van den berg and Rayner, 1995; Schaller *et al.*, 2011). Digit loss is the complete loss of a digit, while digit reduction is the reduction in size of a digit to a point where they are usually vestigial. Digit loss or reduction can take place during the patterning process where the temporal and spatial expression of patterning genes are altered in a way which results in fewer digits. This process can also take place after patterning where already established digit primordia are lost via programmed cell death.

While certain vertbrates undergo digit loss or reduction, other vertebrates maintain the pentadactyl state. An example of a pentadactyl vertebrate with modified limbs is the aye-aye (*Daubentonia madagascariensis*). The aye-aye is a strepsirrhine primate, of the lemuroidea superfamily which is native to Madagascar (Groves, 2001). The fore limb of *D. madagascariensis,* possesses 5 digits, and has become modified for the purposes of foraging and feeding, particularly the autopod (Milliken, Ward and Erickson, 1991)(Figure 3A). The autopod makes up 41% of the total length of the forearm and the forth digit makes up 71% of the autopod (Jouffroy *et al.*, 1993). The third digit is of particular interest as it is long and extremely narrow. The aye-aye uses this digit as a foraging tool to remove larvae from trees

(Erickson, 1994). No research has been done on aye-aye limbs; however given the role that fibroblast growth factors play in limb development, it may be that the prolonged expression of these genes are responsible for the elongated nature of the aye-ayes forelimbs (Niswander *et al.*, 1993; Cohn *et al.*, 1995; Crossley *et al.*, 1996; Martin, 1998; Kawakami *et al.*, 2001; Sun, Mariani and Martin, 2002; Logan, 2003).

Bats are mammals, capable of true and sustained flight (Taylor, Nudds and Thomas, 2003). They achieve this with the use of their membraneous wings, formed by modified forelimbs, which have 5 digits. The most notable modification is the drastic elongation and narrowing of digits II-V and the retention of the interdigital membrane (Figure 3B). These anatomical properties are a result of altered *Shh* expression. *Shh* expression is altered such that its release is delayed, and later in development, its expression is reinitiated in the interdigital regions. The later *Shh* expression is accompanied by *Fgf8* expression, also in the interdigital regions, creating a positive feedback loop. It is this *Shh-Fgf8* feedback loop which promote growth of the phalanges and interdigital tissue retention because of the upregulation of *Gremlin* by *Shh* (M.K. Khokha *et al.*, 2003; Hockman *et al.*, 2008).

Ducks are waterfowls of the family Anatidae. They posses four toes on their hind limbs with webbing between digits II, III and IV. Similar to bats, the webbing between duck hindlimb digits is a result of persistant *Gremlin* expression in the interdigital region at late limb development. GREMLIN is a *Bmp* inhibitor, which drives interdigital programmed cell death (PCD) (Merino *et al.*, 1999). A reduction in *Msx1* and *Msx2* expression is also observed (see below) (Gañan *et al.*, 1998).

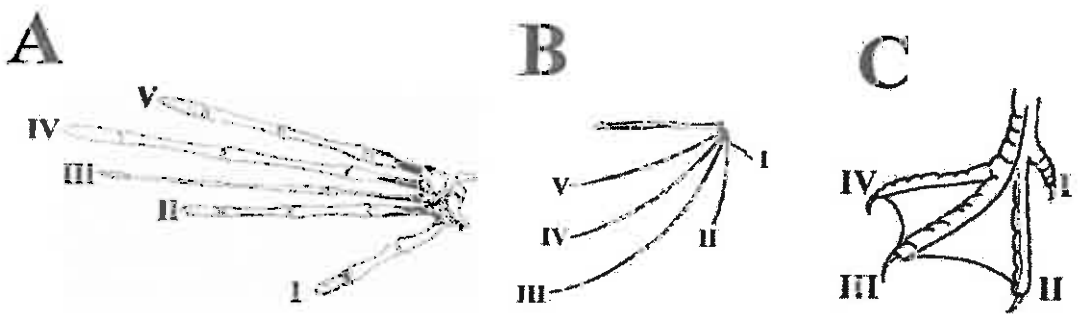

Figure 3 Modified limbs of the aye-aye, bat and duck. 3A) The skeletal limb structures of the aye-aye where the elongated and narrowed third digit can be seen. 3B) The skeletal limb structures of the bat where the elongation of digits II-V can be seen. Not pictured are the interdigital membranes which are retained. 3C) Is the hind limb of the duck with the webbing between II, II and IV.

1.3 Digit Loss and Reduction

As stated above, certain vertebrates under go digit reduction, either during or after the patterning process.

Digit reduction during patterning can be observed in the two-toed ear-less skink (*Hemiergis quadrilineata*) where the early termination of *Shh* expression leads to the development of only digits II and III in the hind limb (Shapiro, Hanken and Rosenthal, 2003). The phenomenon of patterned digit reduction can also be observed in the cow (*Bos taurus*) and pig (*Sus scrofa*) (See below).

A clade of mammals which have less then five digits due to loss of digits are the true ungulates. True ungulates were historically distinguised by their hooves, but the clade has been expanded to include non-hooved mammals such as whales. This clade is further sub divided into two orders: Artiodactyla, or even toed ungulates, and perissodactyla, or odd toed ungulates. Atriodactyla include mammals of the family bovidae, camelidae, cervidae, and tayassuidae;

and perissodactyla include mammals of the family rhinocerotidae, equidae and tapiridae (Martin, Pine and DeBlase, 2001).

Developmental studies have not been done on the limbs of many ungulates, but among those which have been studied are *Bos taurus* and *Sus scrofa.* Both *B. taurus* and *S. scrofa* posses paraxial limbs, meaning that the main weight-bearing digits are digits III and IV, which have given rise to cloven hooves, while digits II and V have become vestigial and digit I is not present. Digit reduction in *B. taurus* occurs during the autopod patterning process. The oligodactyly of *B. taurus* is a result of a change to a *Ptch1* cis-regulatory module causing *Ptch1* expression to be more posteriorly restricted. This alters the distribution of Shh throughout the limb bud mesenchyme, as well as and subsequent Shh targets such as Gli3 and *Hoxd* gene products, to a more uniform state (Lopez-Rios *et al.*, 2014). The exact mechanism of digit reduction in *S. scrofa* has not been elucidated, however it was found the *Ptch1* expression was posteriorly restricted and no increased cell death in the developing limbs is observed (Sears *et al.*, 2011).

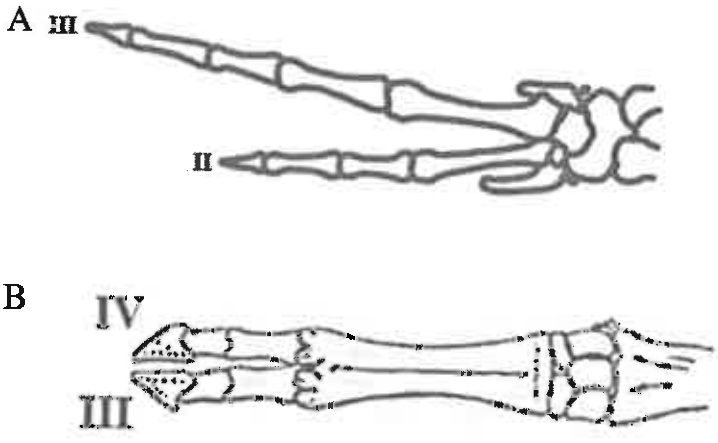

Figure 4 The skeletal limb structures of vertebrates whose limbs are shaped by events during limb patterning. 5A) The limb of the two-toed earless skink (*H. quadrilineata*) with only digit II and III as a result of early *Shh* termination. 5B) The hindlimb of the cow (*B. Taurus*) with two symmetrical digits; III and IV, resulting from alterations in the *Ptch1* cis-regulatory module

Digit loss post patterning occurs in the three-toed jerboa (*Dipus sagitta*) where Digit I and V are eliminated after patterning by programmed cell death (Cooper *et al.*, 2014). Cooper et al., 2014 noted that the developing hind limb bud of early *D. sagitta* embryos possessed five digit precursors which are eradicated later in development. They found expanded *Msx2* expression in the domains of digits I and V as well TUNEL positive nuclei. A similar mechanism was observed in the horse, where the weight bearing digit is digit III and digit II and IV become vestigial. An increase in *Msx2* expression in the anterior and posterior of the limb is seen. Also observed were TUNEL positive nuclei around digit III, overlapping with the presumptive digit II and IV primordia coinciding with the expanded *Msx2* expression. Similar observations are made in the developing limbs of the camel, whose weight bearing digits are III and IV and digits II and V are vestigial. In the camel limb bud, apoptosis is observed in the regions flanking digits III and IV where digits II and V would have formed and the expansion of *Msx2* is observed (Cooper *et al.*, 2014). Using *Sox9* probes, De Bakker et al.,2013 showed that several bird species, including the ostrich, emu, chicken, barbary dove and zebra finch, as well as the crocodile, display precartilage markers during development of digits which do not develop into fully ossified digits in the adult. They also found that posteriorly expressed genes, such as *Shh, Hoxd11* and *Hoxd12,* are conserved in the specimins that were studied. Conversely, anteriorly expressed genes, like *Gli3* and *Alx4,* show variation in their expression

1.4 Programmed Cell Death During Limb Development

Programmed cell death is a genetically controlled process where cells are destroyed in a coordinated manner in order to sculpt tissue, and eliminate damaged or harmful cells (Hernández-Martínez and Covarrubias, 2011). Three different types of PCD have been described according to the molecular machinery involved and the morphologies the cells acquire during the process: Type I known as apoptosis, type II known as autophagy and type

III known as lysosomal cell death (Clarke, 1990). Interdigital cell death is a result of caspase mediated and intrinsic apoptosis, and lysosomal mediated cell death (Zuzarte-Luis *et al.*, 2006, 2007). Caspase mediated cell death can be a result of either the activation of death receptors or the release of cytochrome *c* (Hengartner, 2000).It has been observed that that the introduction of a caspase inhibitor reduces apoptosis, but does not completely eliminate it, this suggests mechanistic redundancy (Chautan *et al.*, 1999). Lysosomal cell death is mediated by lysosomal cathepsins regulated by BMP signalling. The mechanisms of lysosomal cell death include nuclear translocation of apoptosis-inducing factors and mitochondrial permeabilisation (Zuzarte-Luis *et al.*, 2007). It has also been observed that interdigital cell death is preceded by DNA damage. The cause of the damage is unknown, but one suspected cause is oxidative stress from reactive oxygen species. Another is the alteration in chromatin configuration by high mobility transcription factors (Montero *et al.*, 2016). Cell senescence has been observed among cells destined to be eliminated in the interdigital tissue of chickens. Several tumour suppressor genes and markers of cell senescence including *p21* and *Btg2* are expressed in the interdigital tissue (Lorda-Diez *et al.*, 2015).

Developmental studies and PCD go hand in hand as one of the best models of PCD is the developing limb because of the association of tissue degeneration and cell death. PCD has been extensively studied in the developing limbs of the mouse and chicken (Mori *et al.*, 1995; Yokouchi *et al.*, 1996; Jacobson, Weil and Raff, 1997; Macias *et al.*, 1997)

During limb development the first area of apoptosis detected in the developing chicken limb takes place at Hamburger and Hamilton stage 21 (HH21), in the anterior region of the limb bud known as the anterior necrotic zone (ANZ) (Hamburger and Hamilton., 1951). This takes place to eliminate the tissue anterior to the first digit, digit I in the chicken. This is followed by apoptosis of the limb bud mesenchyme situated at the posterior end called the posterior necrotic

zone (PNZ) at stage HH24. Interdigital cell death (ICD) occurs at stage HH30 in the developing chick limb bud (Hamburger and Hamilton., 1951). Interdigital cell death, as the name would suggest, occurs as the mesenchymal tissue in between the forming digits is eliminated by apoptosis.

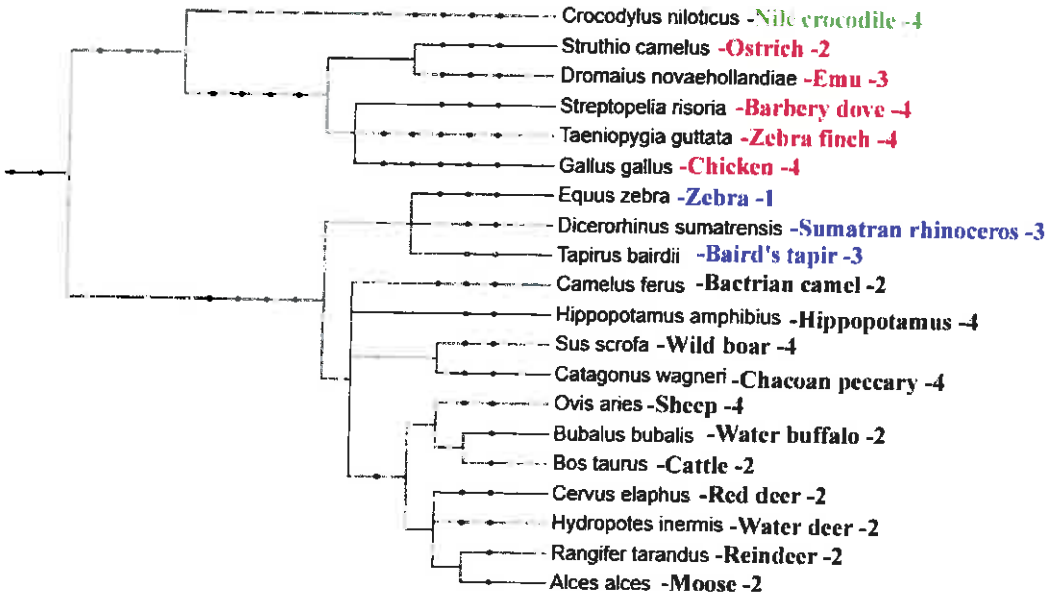

Figure 5A A phylogenetic tree of oligodactylous vertebrates. Displayed are the scientific names, common names and number of digits in their hind limbs. Those in green are Reptiles, red are birds, blue are odd toed ungulates and black are even toed ungulates. Phylogenetic tree generated by PhyloT, Biobyte solutions GmbH 2016, available at http://phylot.biobyte.de/index.html

Figure 5B Images of the limbs of the oligodactylous limbs in the phylogenetic tree of figure 5A. A- Nile crocodile (4 digits in hind limb), B- ostrich (2), C- Emu (3), D- Barbery dove (4), E- Zebra finch (4), F- Chicken (4), G- Zebra (1), H- Sumatran rhinoceros (3), I- Baird's tapir (3), J- Camel (2), K- Hippopotamus (4), L- Wild boar (4), M- Chacoan peccary (4), N- Sheep (4), O- Water buffalo (2), P- Cattle (2), Q- Red deer (2), R- Water deer (2), S- Reindeer (2), T- Moose (2). Image sources are listed in appendix B.

1.5 Apoptotic Genes

1.5.1 Bmp4

Bone morphogenetic proteins (Bmps) are a member of the transforming growth factor-β (TGF-β) family, which are intrinsic in many developmental pathways and may play a role in ICD (Kingsley, 1994). Bmp's are necessary for AER formation and maintenance, as well DV axis formation upstream of *En1* (Pizette, Abate-shen and Niswander, 2001). Bmp4 regulates the Fgf/Shh feedback loop by down regulating Fgf activity. Bmp4 down regulates Fgf expression, restricting the AER to the ectodermal apex of the limb bud. This feedback loop is further regulated by the Bmp antagonists: Gremlin and Noggin (Wang *et al.*, 2004; Bénazet and Zeller, 2009).

Bmp's induce cellular responses by binding with their specific serine/threonine kinase receptors, and the intracellular signal transduction is mediated by SMAD proteins (Massagué, Seoane and Wotton, 2005; Marom *et al.*, 2011). Bmp4 signals are carried out by BmpR-IA, the disruption of which emulates *Bmp4* deletion (Ahn *et al.*, 2001).

The role of Bmps in digit specification is displayed by the resultant polydactylous limbs with multiples of the same digit when treated with Noggin and Bmp antibodies (Drossopoulou *et al.*, 2000). *Bmp2, 4, 5* and *7* expression has been observed in the interdigital mesenchyme during ICD (Geetha-Loganathan *et al.*, 2006). The role of *Bmp4* in ICD was suggested by the observation that local application of Bmp4 to a chick limb bud accelerates ICD in the interdigital regions (Gañan *et al.*, 1996). Conversely, the introduction of Bmp2 and -4 receptors lacking a cytoplasmic domain into the developing chick limb tissue results in webbed limbs (Yokouchi *et al.*, 1996). In a similar experiment, a dominant negative type I Bmp receptor used to block Bmp signalling was accompanied by a decrease in *Msx2* expression in chick

limbs in addition to a reduction in ICD (Zou and Niswander, 1995). This is also supported by the observation that inactivation of *Bmp2* and *Bmp4* in the mouse limb reduces ICD and leads to mild syndactyly (Maatouk *et al.*, 2009).

However, Bmp expression does not always correlate with ICD at all developmental stages, both temporally and spatially. Additionally, Bmps are secreted factors and gene expression patterns are inadequate in establishing functional correlation (Hernández-Martínez and Covarrubias, 2011).

1.5.2 Msx1 and Msx2

Msh homeobox Msx genes are a sub-family of genes which contain the homeodomain motif and are expressed in a number of vertebrate tissues during development including neural crest derivatives, cranial sensory placodes, mammary glands, hair follicles, teeth and limbs (Davidson, 1995; Chen *et al.*, 1996; Bendall and Abate-Shen, 2000). Msx1 and Msx2 are transcription factors expressed in the interdigital mesenchyme, suggesting participation in ICD (Gañan *et al.*, 1998). Ectopic expression of *Msx2* has been shown to promote apoptosis and also induce *Bmp4* expression (Ferrari *et al.*, 1998). *Msx1* and *Msx2* are required to specify proper digit identity and number through *Shh* and *Bmp4* signalling pathways (Bensoussan-Trigano *et al.*, 2011). Mice with null mutations in either *Msx1* or *Msx2* have normal limbs, suggesting a functional redundancy between these two gene. As expected *Msx1/2* double mutants show a multitude of limb malformations implicating *Msx1* and *Msx2* in the formation of all three axes. These malformations include shorter limbs lacking anterior skeletal elements, no specification of the dorso-ventral boundary in the anterior ectoderm and therefore no AER formation resulting in anterior oligodactyly. Extended *Fgf* expression in the posterior portion

of the developing limb, as a result of *Msx1/2* double knockout, can result in polydactyly (Lallemand *et al.*, 2005).

Mxs2 expression is controlled by Bmp signal transduction through a Bmp cis-regulatory element located in the *Msx2* promoter (Brugger *et al.*, 2004). Msx1 expression is regulated by Bmp as well as other pathways.

Many studies have demonstrated an interaction between *Msx2* and *Bmp4* in the PCD pathway (Graham *et al.*, 1994; Zou and Niswander, 1995; Marazzi, Wang and Sassoon, 1997). An up-regulation of Bmp4 leads to an upregulation of Msx2 and in turn an increase in programmed cell death. Reduced expression of *Msx1* and *Msx2* is observed in the interdigital region in the duck hind limb where the interdigital region persists and results in webbing. Application of exogenous Fgf to the interdigital region results in an increased expression of *Msx2* and a consequent increase in Bmp-induced cell death (Gañan *et al.*, 1998).

As mentioned above, the developing ostrich limbs displays 5 precartilage digit primordia in early development, but only digits II, III and IV in the fore limb and III and IV in the hind limb develop into fully ossified digits. The presence of these digit primordia indicate that PCD, post patterning, may be the mechanism of digit loss (de Bakker *et al.*, 2013).

The ostrich is a precocial bird and therefore undergoes a longer period of tissue maturation during its 42 day incubation period (Starck and Ricklefs, 1998; Brown and Prior, 1999). Although twice as long, the embryonic development of the ostrich is comparable to the development of the chicken as documented by Hamburger and Hamilton, 1951, and no significant difference have been found. After 7 days of incubation the embryo has turned onto its side and the eyes have a faint grey colour. At 14 days the beak and vascular system has formed and grooves between the digits are distint. By the 21st day of incubation feathers and

eaylids have formed. Claws havr developed by day 28 and a thick coat of feathers has grown by day 35 (Brand *et al.*, 2017).The highest survival rate among artificially incubated ostrich eggs are those stored at at 17°C for 3-4 days after collection, and then incubated vertically, with the air sac on top, at 36°C (Van Schalkwyk *et al.*, 1999; Brand *et al.*, 2012).

It is hypothesised that digit loss in the *Struthio camelus* hind limb during development occurs due to post patterning mechanisms, specifically Msx and Bmp-mediated program cell death.

The aim of this study is to determine the molecular mechanisms of digit loss in *Stuthio camelus*. This occurrence will be investigated from a post-patterning, programmed cell death aspect using the *Gallus gallus* embryo as a control. The primary candidate genes to be investigated are *Bmp4* and *Msx2*. These two genes are confirmed to play a role in programmed cell death in vertebrates. Other genes under investigation are *Msx1* and *Bmp2,* homologs of the primary gene candidates, as well as *Shh, Sox9,* and *Fgf10,* genes known to play a role in shaping the developing limb bud.

2.Materials and Methods

2.1 Tissue Dissection

Chicken and ostrich limb bud tissue was dissected from freshly incubated eggs at the appropriate developmental stages. Ethical clearance was obtained to perform this work (clearance certificate number: 2015/05/21/O). Chick embryos were staged according to convention set by Hamburger and Hamilton (Hamburger and Hamilton., 1951). Because the ostrich incubation period is twice as long as that of the chick, an approximate staging system was used for ostrich embryos wherein the incubation times for a particular chick stage was doubled for the corresponding ostrich stage, designated: SCHH stages. As such a *G. gallus*

embryo at stage HH6, will have incubated for 24 hours, and a *S. camelus* embryo at stage SCHH6 will have incubated for 48 hours. Both ostrich and chicken eggs were incubated at 37°C.

2.2 Nucleic Acid Extraction

Nucleic acid extraction was performed on freshly dissected tissue using the NucleoSpin RNA Kit (Macherey-Nagel) for RNA and NucleoSpin Tissue kit (Macherey-Nagel) for DNA. Both kits require the lysing of the sample tissue, adjusting the DNA binding conditions with ethanol, binding the DNA to a silica membrane, washing, and eluting the sample. The NucloeSpin RNA Kit required a DNA digestion step before the washing step. To verify the success of the nucleic acid extraction and agarose gel was run. All agarose gels were 1% agarose gels ran at 8V/cm.

2.3 Whole Mount *In Situ* Hybridisation

2.3.1 RT-PCR

In preparation for whole mount *in situ* hybridisation, RNA probes were synthesised from cDNA contained in plasmids. cDNA synthesis was performed with the cDNA synthesis RevertAid First Strand cDNA synthesis kit (Thermo Scientific). OligoDTs and sequence specific primers (SSP's) were used to amplify the genes of interest. A positive control was done using GAPDH control RNA and GAPDH SSPs and a no template negative control was done. The reactions were incubated at 42° for 60 minutes. The genes were then amplified by PCR with the SSPs.

2.3.2 PCR

Bmp4 was amplified by PCR using the product of the RT-PCR as the template and sequence specific primers. The primers for *G. gallus Bmp4* amplification had the following sequences, forward primers: GGTCATCCTACTATGCCAAG, reverse primer: CGGCTTCATCACTTCGTAAA. The primers gave a product of 535 base pairs. The PCR protocol was as follows: An initial denaturing step of 94°C for 3 minutes, followed by a 30 second denaturing step at 94°C, a 30 second annealing step at 49°C, followed by a one-minute elongation step at 72°C. these three step were repeated 35 times followed by a final elongation step of 1 minute. KapaTaq Master Mix (Kapa Biosystems) was used to perform this PCR protocol as per product guidelines with a primer concentration of 300nM for both primers. The PCR products were purified with the GeneJet PCR purification kit (ThermoScientific).

2.3.3 Cloning

The *Bmp4* amplicon was then ligated into the pGEM-T Easy Vector. *Escherichia coli,* strain JM109, was transformed, by heat shock, with the vectors containing *Bmp4, Bmp2, Shh,* and *Fgf10.* The transformed cells were plated on LB plates supplemented with ampicillin, IPTG and X-gal. After an overnight incubation at 37°C, white colonies were picked and cultured overnight at 37°C in LB broth supplemented with ampicillin. The vector was then isolated from the cell culture with the Plasmid Mini-prep kit (Zymogen). The cells were pelleted by centrifugation, lysed and the cell debris was separated from the nucleic acid by centrifugation. The nucleic acid was bound to the silica membrane, washed and the plasmid eluted.

The plasmids were sequenced by Inqaba Biotech to confirm the identity and direction of the insert. The plasmids which yielded positive results were used to synthesise probes.

2.3.4 Probe Synthesis

RNA probes for *Msx1*, *Msx2* and *Sox9* were already synthesised by past students. While templates for *Bmp2*, *Shh* and *Fgf10* were provided in vectors by Dr N. Nikitina. Probes were synthesised for *Bmp4*, *Bmp2*, *Shh*, and *Fgf10*. All the probes were of *G. gallus* origin.

Dependent on the vector and the orientation of the insert, the plasmids were linearised with an appropriate restriction enzyme and either SP6, T7, or T3 RNA polymerase was used to synthesise the RNA probes with digoxygenin labelled UTP (Table 1).

Each probe synthesis reaction contained 4.0µl of 5x Transcription buffer (Thermo Scientific), 2.0µl of RNA polymerase (Thermo Scientific), 2.0µl of 10x DIG RNA labelling mix (Roche), 0.5µl of RNASin RNase inhibitor (Thermo Scientific), 1µg of linearised plasmid and the volume made up to 20µl with DEPC H_2O. The probe synthesis reactions were incubated at 37°C for 60 minutes after which an additional 2.0µl of RNA polymerase was added, and incubated for another 60 minutes at 37°C. 2.0µl of DNase (Thermo Scientific) and 2.0µl of DNase buffer (Thermo Scientific) was then added to each reaction to digest the DNA template. The reactions were then incubated at 37°C for 1 hour.

Gene probe template	Restriction enzyme	RNA polymerase
Bmp2	ApaI	T3
Bmp4	ApaI	SP6
Fgf10	SalI	T3
Shh	Ecor32I	T3

Table 1 Shows which restriction enzyme were used to linearise the plasmids containing the probe template as well as the RNA polymerase used to transcribe the RNA probe.

This reaction was purified with the NucleoSpin RNA cleanup kit (Macherey-Nagel). 50µl of the purified product was diluted with 1950µl of hybridisation mix with tRNA (Appendix A) to create a stock solution. Before use, this stock solution was further diluted, 1:4, with tRNA hybe mix to create the RNA probe mix working solution. Before use, embryonic tissue is incubated for 3 hours at 70°C in the working solution to remove excess tRNA from the working solution.

2.3.5 Whole-mount *In Situ* Hybridisation

To visualised the expression of the selected genes, whole-mount *in situ* hybridisation (WISH) was performed on *G. gallus* and *S. camelus* hind limbs with *Bmp2, Bmp4 Msx1, Msx2, Sox9, Fgf10* and *Shh* probes all of *G. gallus* origin. The *G. gallus* probe templates were similar enough to the *S. camelus* mRNA to use on both organisms. The *G. gallus Msx1* probe had a 94% similarity to the *S. camelus* mRNA, the *Msx2* probe has a 91% similarity to *S. camelus* mRNA. WISH was performed on *G. gallus* limb buds using *Fgf10, Shh, Bmp1, Bmp2, Msx1,Msx2* and *Sox9.* WISH was performed on *S. camelus* limb buds using only *Msx1* and *Msx2* because of the limited amount of fertilised eggs available.

The limb tissues used were harvested from freshly dissected embryonic tissue. The limb buds were fixed in 4% PFA in PBS (Appendix A) at 4°C, overnight. All subsequent washes were carried out at room temperature and on a shaker at 50 rpm, unless otherwise specified. The PFA was removed and the limb buds were washed trice for 5 minutes in DEPC treated PBST. For storage the limbs were dehydrated into methanol with a series of 5 minute washes in 25% methanol in DEPC-PBST, 50%, 75% and 100% methanol.

The limb buds used for whole mount *in situ* hybridisation were rehydrated to PBST with a series of washes. Once hydrated into 100% DEPC-PBST the limb buds were again washed trice for 5 minutes in DEPC-PBST. The limb buds were then treated with 10µ/ml proteinase K in DEPC-PBST for 30 minutes, followed by 10 minutes in 2mg/ml glycine in DEPC-PBST,

both without shaking. The limb buds were then washed twice with DEPC-PBST for 5 minutes, without shaking. The limb buds were fixed in 4% PFA and 0.2% glutaraldehyde in DEPC-PBST for 20 minutes, without shaking, followed by 4 five minute washes in DEPC-PBST, with shaking.

The limb buds were washed in a 1:1 mix of DEPC-PBST and tRNA hybe mix for 10 minutes, followed by two washes, five minutes each, in 100% tRNA Hybe mix. The tRNA hybe mix was replaced with the RNA probe mix and the limb buds were incubated at 70°C overnight.

The RNA probe mix was removed and the limb buds were washed twice in hybridisation mix without tRNA for 15 minutes at 70°C, followed by four washes, 30 minute each in hybe mix at 70°C. The limb buds were then washed for 30 minutes in a 1:1 mix of hybe mix and MABT, followed by four washes of 30 minutes in MABT at room temperature. The limb buds were washed in a blocking solution comprised of 3% BSA in MABT at room temperature first for 15 minutes, then for one hour. There after the limb buds were washed in the antibody solution, Anti-digoxygenin-AP Fab fragments (1:1000) with 3% BSA in MABT at room temperature for 5 minutes then overnight at 4°C.

The antibody solution was removed and the limb buds were washed in MABT at room temperature: twice for five minutes, twice for 30 minutes and six times for one hour, there after they were washed overnight at 4°C in MABT (Appendix A).

The limb buds were removed from the MABT and washed twice in 100mM tric-Cl (pH 9.5) for 15 minutes, then again in NTMT (Appendix A) for 15 minutes, four times. The limb buds were then incubated in BM purple in the dark until staining developed.

Once staining had developed, the limb buds were washed twice in 100mM tric-Cl (pH 9.5) for 15 minutes, in the dark, followed by three washes, each five minute in PBST, in the dark. The

embryos were incubated in 4% PFA in PBS for 2 hours at room temperature, followed by 3 five minutes washes in PBST. The limb buds were dehydrated into methanol with a graded series of methanol and PBST (25% methanol in PBST, 50%, 75% and 100% methanol) for storage. For photography the embryos were rehydrated in to PBST and then washed and viewed in a solution of 25% glycerol in PBS.

The embryos were photographed with an Axio Zoom V16 microscope (Zeiss).

2.4 Cell Death Assay

2.4.1 Cryosectioning

The limb buds to be used for the TUNEL assay and ICC were dehydrated in ethanol for storage. Once ready for use the limb buds were rehydrated to PBST with a series of ethanol/PBST washes. The buds were washed a further 3 times in PBST, followed by a five-hour wash in 5% sucrose in PBST at room temperature and an overnight wash in 15% sucrose (PBST) at 4°C. The limb buds were removed from the sucrose solution and incubated in Cryomatrix embedding medium (ThermoScientific) at 4°C overnight. The embedding medium was replaced and the samples were flash frozen in liquid nitrogen and stored at -70°C.

The embedded limb buds were sectioned, with a thickness of 15µm, and mounted on slides. The sections were processed to detect either cell death, cartilage formation, or both. Cell death detection was performed with the cell death assay *in situ* Cell Death Detection Kit (Roche), while cartilage development was done using mouse, anti-Sox9 primary antibody and anti-mouse CF568 secondary antibody (see below).

2.4.2 TUNEL and Immunocytochemistry

The TUNEL assay detects nicks in DNA which are an indication of apoptosis. These nick sites are then labelled with fluorescein. Fluorescein has an excitation wavelength range between 450nm-500nm and a maximum at 490nm and an emission wavelength range between 515nm-565nm with a maximum at 525nm.

Sox9 is involved in cartilage formation and its presence will indicate the formation of digit primordia (Bi *et al.*, 1999). The secondary antibody is conjugated to the fluorophore CF568 which has a maximum excitation wavelength at 562nm and a maximum emission wavelength at 583nm.

The slides prepared previously were washed in PBST for 10 minutes at 42°C to remove the mounting media, followed by two washes of five minute in PBST at room temperature. The tissue sections were fixed in 4% PFA for 20 minutes at room temperature, then washed thrice for 5 minutes in PBS also at room temperature. The slides were then incubated in 10mM sodium citrate (0.05% tween) at 70°C for 30 minutes followed by two washes of five minutes each in PBS at room temperature. 50µl of the TUNEL reaction mixture was added to each slide, which was then covered with parafilm and incubated at 37°C in a humidity chamber in the dark for 1 hour. There after the slides were washed 3 time for 5 minutes in PBS at room temperature. The slides were then incubated in 3% BSA in PBST for 2 hours. The slides were then incubated in mouse, anti-Sox9 primary antibody (5µl/ml) in 3% BSA (PBST) at 4°C overnight in a humidity chamber. The following day, the slides were rinsed six times for 30 minutes in PBST at room temperature. The slides were then incubated in rabbit, anti-mouse CF568 secondary antibody (5µl/ml) in 3% BSA (PBST) at 4°C overnight in a humidity

chamber, followed by six 30 minute washes in PBST at room temperature. The slides were air dried and mounted with CCMount.

The slides were photographed with an Axio Zoom V16 microscope (Zeiss) equipped with an Apo Tome 2 camera (Zeiss). The software used was ZEN 2012 (Zeiss).

2.5 *Msx2* Promoter Analysis

2.5.1 Bioinformatics

At the time that this research was done the *S. camelus* genome had been sequenced, but not yet organised and only existed as a catalogue of WGS contigs. In order to locate the promoter region upstream of the *S. camelus Msx2* gene, a BLAST was performed with the *G. gallus Msx2* sequence (accession: NM_204559.1) against the *S. camelus* genome to locate the *S. camelus* ortholog. Once the ortholog was located the upstream contigs were assembled to create the promoter region.

2.5.2 PCR

In order to isolate the *Msx2* promoter regions, sequence specific primers were designed to be used in PCR with the extracted *S. camelus* gDNA as the template. The sequence of the forward primer was: TTCTACGCTCCAGCATCACG, and the sequence for the reverse primer was: CGAAGCAAGAAAAGAGCCGC. A 3.5KB region upstream of the *S. camelus Msx2* gene was selected. Expand High Fidelity PCR system (Roche) was used for these PCR protocols according to the product guidelines using 300nM of each primer and 250ng of template DNA. The PCR protocol is laid out in table 2. The PCR products were purified with the GeneJet PCR purification kit (ThermoScientific). This kit uses the principle of binding the DNA to a silicate membrane, washing away impurities, and eluting the purified DNA

2.5.3 Cloning

The PCR product was ligated into pTK-EGFP in an overnight reaction at 4°C. The ligation reaction consisted of 5µl of 2X ligation buffer, 1µl of pTK-EGFP plasmid, 1µl of T4 ligase and 3µl of the PCR product. The plasmid was transformed into JM109 competent *E. coli* cell, which were plated on LB agar plates supplemented with ampicillin. Presence of the insert was screened by colony PCR using the same SSP's used to amplify the promoter region. Colony PCR was done with KapaTaq ReadyMix (Kapa Biosystems). The following protocol was used for the colony PCR: an initial denaturing step of 95°C for 3 minutes, followed by a 30 second denaturing step at 95°C, and 30 second annealing step at 54°C, followed by a three-minute elongation step at 72°C. These steps were repeated 35 times which was followed by a three-minute final extension step at 72°C. The colonies which gave positive results were re-cultured and the plasmids extracted with the Zyppy plasmid miniprep kit (Zymogen) and sequenced to confirm the identity. The plasmid containing the *Msx2* Promote region is here forth referred to as pTK-EGFP-Msx.

PCR conditions of *S. camelus Msx2* promoter region			
	Time (seconds)	**Temperature (°C)**	**Cycles**
Initial denaturation	120	94	1
Denaturation 1	15	94	10
Annealing 1	30	55	10
Elongation 1	180	68	10
Denaturation 2	15	94	20
Annealing 2	30	55	20
Elongation 2	180	72	20
Final elongation	420	72	1

Table 2 Shows the PCR conditions for the amplification of the *S. camelus Msx2* Promoter region. The first denaturation, annealing and elongation steps were repeated 10 times before second denaturation, annealing and elongation stages took place.

2.5.4 Electroporation

The pTK-EGFP-Msx plasmids were then used for electroporation. A second, empty plasmid containing red fluorescent protein transcript, pCIG-RFP, was also prepared as a tracer for electroporated cells to track the uptake of the plasmids. pCIG-RPF contains the CAG promoter, able to drive expression in mammals and birds (Okabe et al., 1997). Chicken eggs were opened such to preserve the embryos after 3ml of albumen was removed from the egg with a needle inserted into the blunt end of the egg. The vitelline layer was removed to expose the embryo which was covered in Ringers solution to provide a conductive medium for the electric pulses. The final concentration of both plasmids in the mixture was 1µg/µl and the green dye was in a 1:9 dilution Using pulled glass needles, the plasmid mixture was injected into the lateral plate mesoderm and somite region at stage HH14. the electrodes were

placed on either sides of the embryo and the shocks were administered. The embryos were pulsed 5 times at 30 volts for 50 milliseconds at 1 second intervals with an ECM 830 electroporator (BTX). Ringers solution was used to cover the embryos to prevent drying out, the eggs were sealed with tape and incubated at 37°C for 48 hours to allow for expression. After the incubation period the eggs were opened, the embryos were dissected out and viewed under an Axio Zoom V16 microscope (Zeiss). The embryos were viewed with a the appropriate fluorescent filters in order to detect the EGFP and RFP expression.

3. Results

3.1 Nucleic Acid Extraction

Using the nucleic acid extraction kits, several samples of both RNA and gDNA were extracted. gDNA was extracted from both *G. gallus* and *S. camelus* embryonic tissue (Fig. 6A and 6B) and RNA was extracted from *G. gallus* embryonic tissue (Fig. 6C). The large band and smearing in figure 6A and 6B indicate a successful gDNA extraction. The 2 bands in figure 6C, which is the 18S and 28S ribosomal RNA, indicating a successful RNA extraction. Lanes 2 and 3 in figure 6B are void of bands, indicating an unsuccessful gDNA extraction, attributed to column overloading. The RNA was to be used to synthesis cDNA and RNA probes thereafter, and the gDNA was used to isolate the *Msx2* promoter region.

3.2 *G. gallus Bmp4* Cloning

The extracted *G. gallus* RNA was used to synthesis cDNA (Fig. 7A), which was then used as a template for the PCR amplification of *Bmp4* fragment (Fig. 7B and 7C). The results were as expected. The positive GAPDH control in lane one of figure 7C shows two bands, indicating success. The negative, no template, control resulted in an empty lane indicating that any amplification is that of the desired products. Lanes 3, 4 and 5 also had two bands in them indicating successful synthesis of the desired cDNA.

DNA was used as a template to synthesise the *Bmp4* fragment using the SSP's. The PCR protocol required optimising in terms of the annealing temperate as seen in fig 7B. The optimal annealing temperature was found to be 49°C, seen in lane 1. The annealing temperature used in lane 2 was 52°C, lane 3 was 51°C and lane 4 was 50°C.

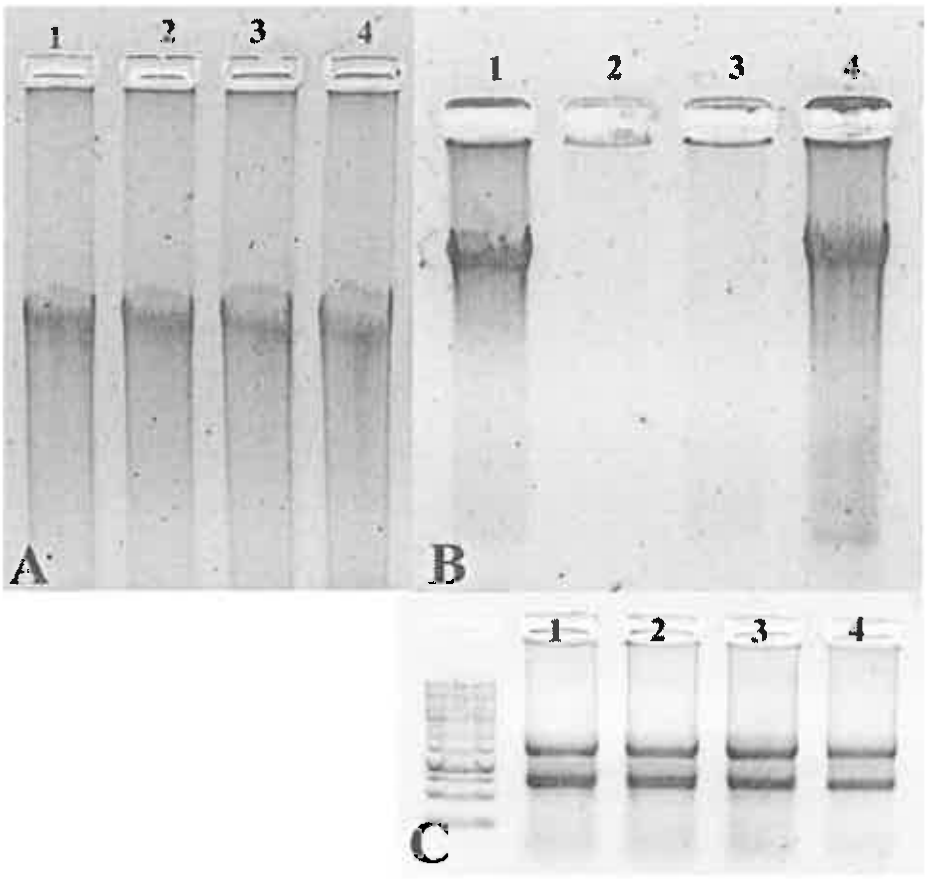

Figure 6 Agarose gel images of nucleic acid extractions. 6A) *G. gallus* gDNA extraction. All four lanes show successful extractions, as evidenced by the smear and single bulbous band. 6B) *S. camelus* gDNA extraction. The samples in lanes 1 and 4 are positive for gDNA while lanes 2 and 3 is negative. 6C)*G. gallus* RNA extraction. The 18S and 28S bands can be seen clearly in all four lanes, indicating success.

The purified PCR product was ligated into the pGEM-T Easy Vector. JM109 *E. coli* were transformed with the ligated vectors containing *Bmp4*, *Bmp2, Shh* and *Fgf10* which were the extracted and sequenced. Once identity was confirmed the vectors were linearised (Fig. 8) and used for probe synthesis. In some cases, multiple banding was observed on the agarose gels. This is attributed to the formation different secondary structures in the case of circular plasmids (fig. 8A and 8C), or the presence of 2 enzyme restriction sites in the case of the linearised plasmid (Fig 8D).

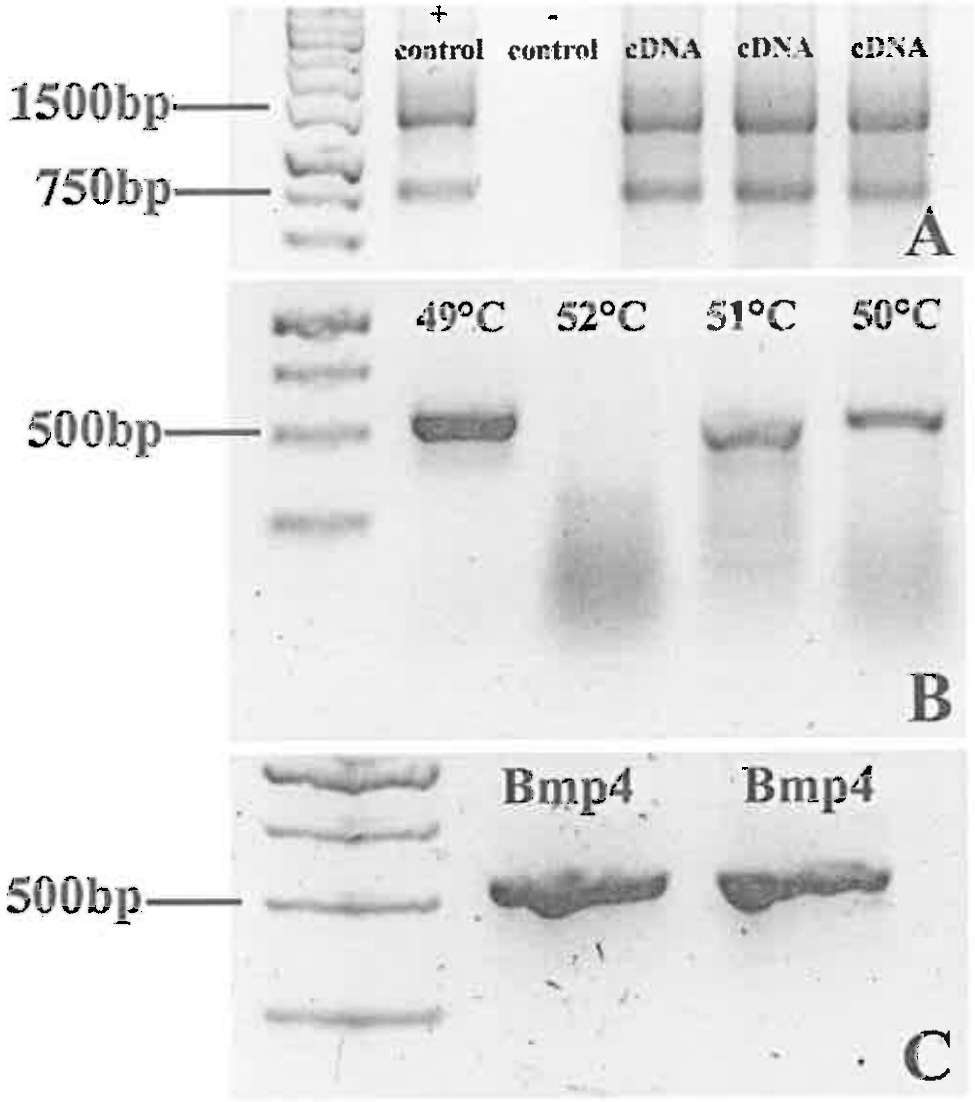

Figure 7 Agarose gels of cDNA synthesis and PCR's of *Bmp4* amplification. 7A) Agarose gel of cDNA synthesis. Lane 1 is the positive control done with GAPDH RNA and GAPDH primers, lane 2 is the no template negative control and lanes 3, 4 and 5 samples amplified with oligo(dT). The presence of 2 bands as in the positive control indicates success. 7B)*Bmp4* PCR optimisation process carried out under varying annealing temperatures. The expected product size was 535bp. 7C) A gel of the optimised *Bmp4* PCR under optimal conditions, 49°C.

3.2 Probe Synthesis

Probes were successfully synthesised for *Bmp2, Bmp4, Fgf10* and *Shh* (Fig.9). The single smeared bands seen for the *Fgf10, Bmp2* and *Shh* probes (Fig. 9) are the RNA probes which remain from the RNA probe synthesis procedure after the DNase digestion step. The darkest band visible on the *Bmp4* lane is the DNA shown before the DNase digestion step. The multiple bands below that are the RNA probes. The multiple bands are likely a result or secondary structures forming within the RNA. The probes were diluted and stored in hybridisation mix with tRNA. Probes for *Msx1*and *Msx2* were synthesised by previous students.

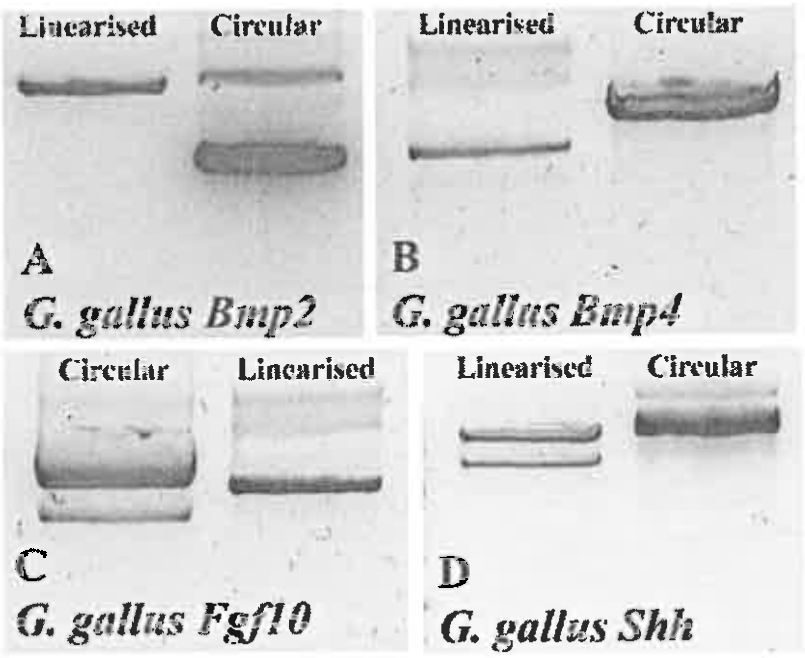

Figure 8 Agarose gels of plasmid linearisations. 8A)Linearisation of the *Bmp2* fragment-containing plasmid with the restriction enzyme ApaI. 8B)Linearised *Bmp4* containing plasmid with ApaI.,8C)Circular plasmid containing the *Fgf10* fragment in lane 1 and the plasmid linearised with SalI in lane 2. 8D)Agarose gel of the *Shh* containing plasmid linearised with EcoR32I.

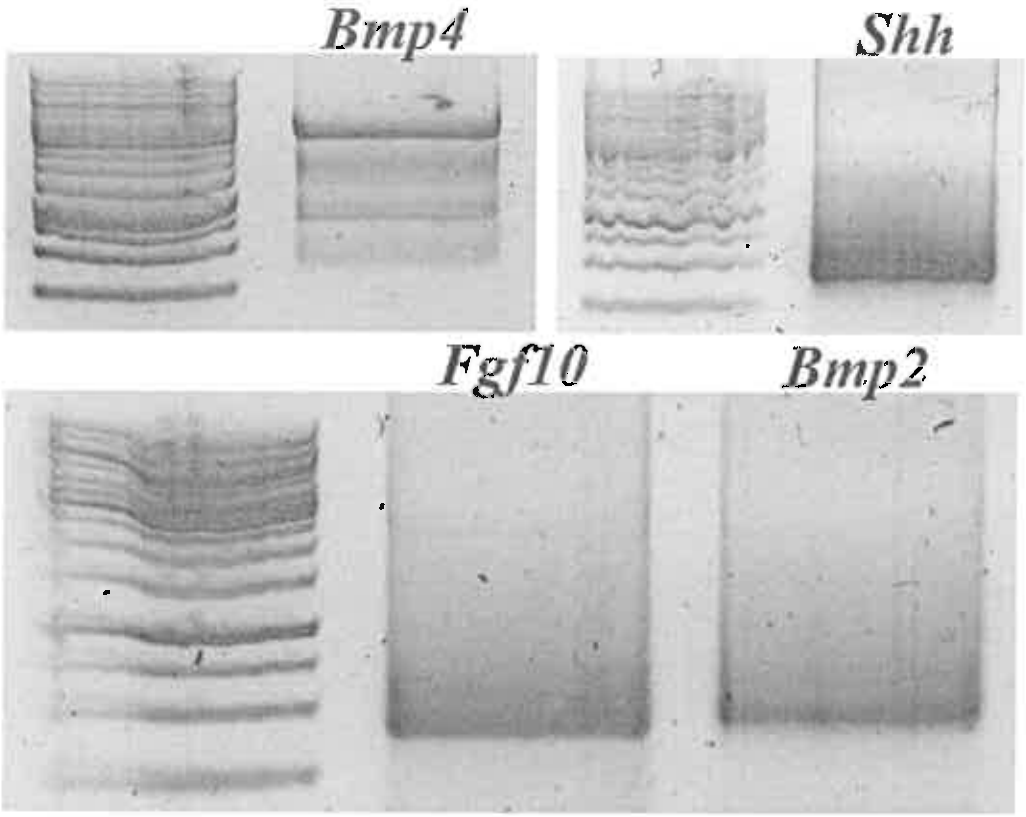

Figure 9 Agarose gels of the synthesised probes. On the top left is the first step of probe synthesis, before DNAse digestion, for the *Bmp4* RNA probe. The darker bands at the top of the lanes are the DNA template, and the fainter bands below that are the RNA probes. The image on the top right shows the RNA probe of *Shh* after DNase digestion of the DNA template. On the Bottom left is a gel image after step 2 of probe synthesis for the RNA probes of *Fgf10* and Bottom right is that of *Bmp2*. The bands visible in the gel are the RNA probes of the respective gene

3.3 Whole Mount *in situ* Hybridisation

Using the synthesised probes, as well as the probes provided by previous students, WISH was performed on the hind limb buds of both *G. gallus* and *S. camelus*.

3.3.1 *Bmp* expression

The expression of *Bmp2* and *Bmp4* in *G. gallus* hind limbs can be observed in the interdigital regions as expected; given their association with *Msx* and PCD (Fig. 10). All limb images are positioned with the anterior (digit I) of the limb at the top of the image, the star marking digit III. At stage HH24, five digit primordia can be distinguished (Fig. 10A). By stage HH25 (Fig. 10B) the expression of *Bmp2* has expanded to the fifth digit primordia. Four digit primordia can be observed in the *G. gallus* limb treated with the *Bmp4* probe at stage HH25 (Fig. 10C). The staining is faint due to low probe concentration.

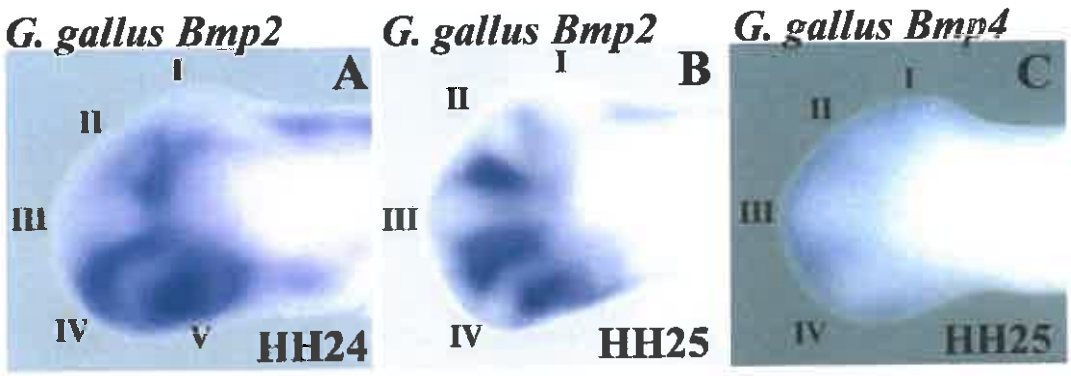

Figure 10 Images of *G. gallus* hind limbs treated with *Bmp2* (A and B) and *Bmp4* (C) probes during WISH.10A) *Bmp2* expression in the hind limb of *G. gallus* can be observed in the interdigital regions where PCD takes place. All five digit primordia are made visible by the staining at stage HH24.10B) by stage HH25 the expression of *Bmp2* remains in the interdigital region however the expression has expanded to the fifth digit primordia, which is eliminated.10C) *Bmp4* expression in *G. gallus* hind limbs also occurs in the interdigital regions, which can be observed between the digit primordia.

3.3.2 *Msx* Expression

Msx1 expression in *G. gallus* hind limbs can be observed in the interdigital region. At stage HH23 (Fig. 11A) the primordia of digits I and II cannot be clearly distinguished, and the primordia of digits III, IV and V are clearly visible. At stage HH24 (Fig. 11B) digit I and II primordia are still not visible, but digits III, IV and V are. However the digit V primordium is beginning to regress as *Msx1* expression expands into that region. By stage HH25 (Fig. 11C) digit II primordium is visible with the digit I primordium becoming apparent and the digit primordium V no longer visible.

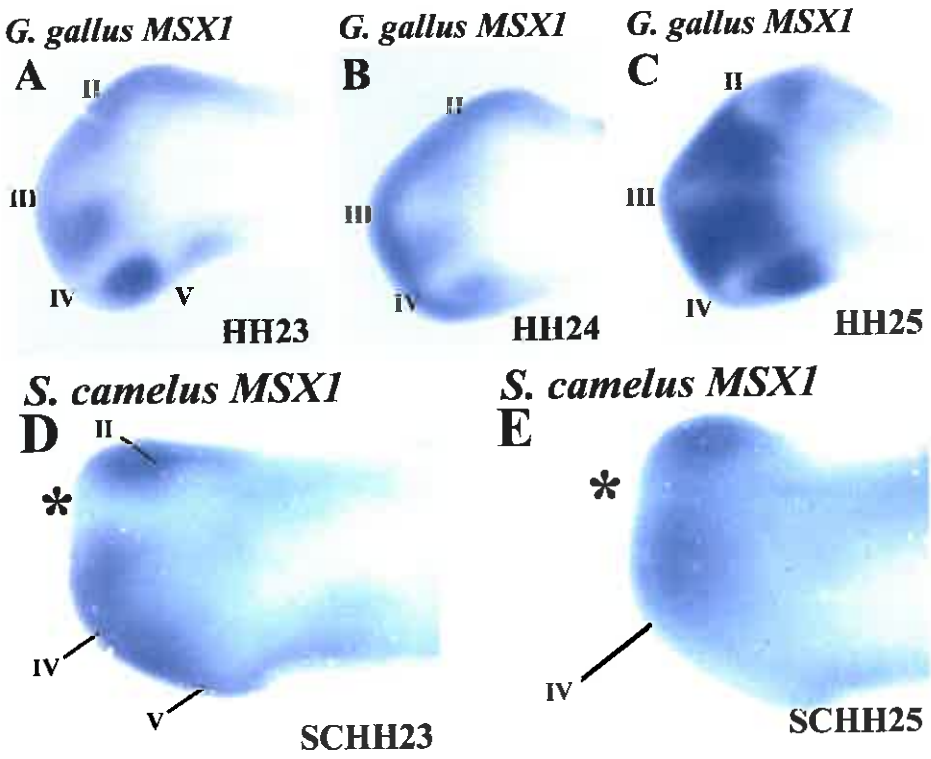

Figure 11 Hind limbs of both *G. gallus* (A, B and C) and *S. camelus* (D and E)treated with the *Msx1* probe during WISH. *Msx1* is expressed in the interdigital regions in the hind limbs of both *G. gallus* and *S. camelus*. The digit primordia are made visible by the staining. 11A) In *G. gallus* digit primordia III, IV and V are distinguishable at stage HH23 while digit primordia I and II are not. 11B) at stage HH24 digit I and II are becoming more visible. 11C) by stage HH25 Digit primordia V is no longer visible and digit primordia I and II are apparent. 11D) In *S. camelus* at stage SCHH23 digit primordia II, III, IV, and V are distinguishable and 11E) by stage SCHH25 only digit primordia III and IV are visible.

Msx1 expression in *S. camelus* is less clear. At stage SCHH23 digit primordia II, III, IV and V can be distinguished (Fig. 11D). By stage SCHH25 only digit primordia III and IV can be distinguished (Fig 11E).

Msx2 expression in *G. gallus* and *S. camelus* hind limbs is also seen in the interdigital regions. The expression pattern of *Msx2* in *G. gallus* at stage HH24 make digit primordia I-IV visible (Fig. 12A), comparable to *Msx1* expression in the *G. gallus* at stages HH24 and HH25. *Msx2* expression in the interdigital regions in *S. camelus* hind limbs at stage SCHH23 makes digits II-V apparent (Fig. 12B). By stage SCHH25 only digit primordia III and IV are clearly visible, with the remnants of digit primordia II and V regressing into the PNZ and ANZ where *Msx2* expression is seen (Fig. 12C).

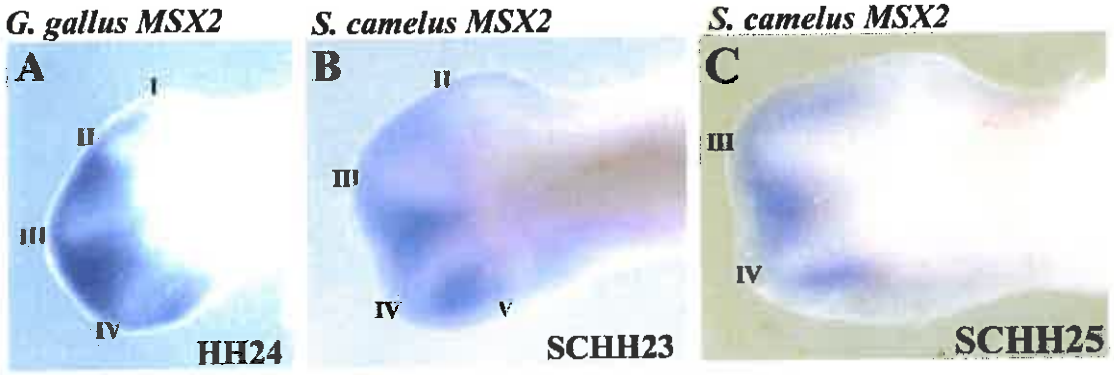

Figure 12 The hind limbs of *G. gallus* (A) and *S. camelus* (B and C) treated with the GG *Msx2* probe during WISH. 12A) The *Msx2* staining in the interdigital spaces of the *G. gallus* hind limb at stage HH24 makes digit primordia I, II, III and IV visible. 12B) At stage SCHH23, the *Msx2* expression in the *S. camelus* hind limb makes digit primordia II, III, IV, and V distinct, 12C) and by stage SCHH25, only digit primordia III and IV are visible.

3.3.3 Expression of Additional Genes

WISH was performed only on *G. gallus* hind limbs with *Fgf10, Sox9* and *Shh,* due to the limited supply of *S. camelus* eggs. The primordia of digit II-V are visible with *Sox9* staining in the *G. gallus* hind limb at stage HH25 (Fig. 13F). *Shh* expression can be seen in the posterior of the *G. gallus* hind limb at stage HH21 (Fig. 13E). *Fgf10* expression in *G. gallus* hind limb can be seen in the distal border of the limb bud at stage HH21 (Fig 13A), expression then expands proximally and to the anterior and posterior regions of the bud (Fig. 13B). By stage HH24, *Fgf10* expression is localised to the developing digit primordia (Fig. 13C) and can be observed

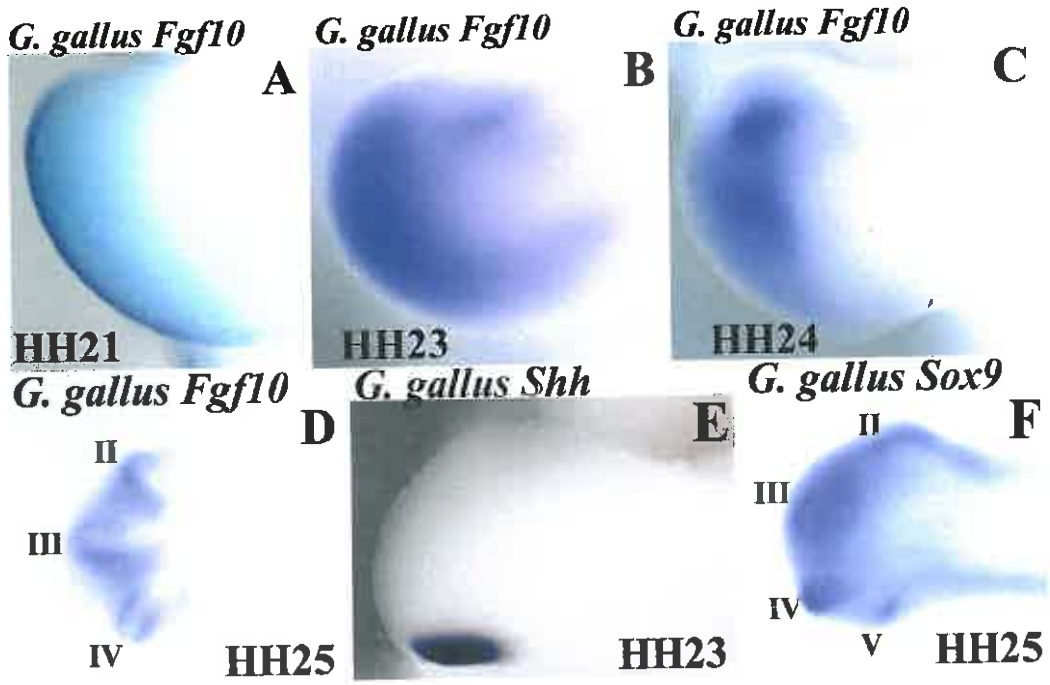

Figure 13 Hind limbs of *G. gallus* treated with the GG *Fgf10,* GG *Sox9* and GG *Shh* probes during WISH. 13A) At stage HH21 *Fgf10* is expressed in the AER of the developing limb bud. 13B) By stage HH23 expression has expanded to the anterior and posterior regions of the limb bud 13C) At stage HH24 *Fgf10* expression is localised to the forming digit primordia. 13D) At stage HH25 *Fgf10* is expressed in the margin of digit II, III and IV digit primordia and interdigital regions. 13E) *Shh* is expressed at the posterior of the *G. gallus* hind limb at stage HH23.13F) *Sox9* is expressed in cartilage precursors at stage HH25 making digits II, III, IV and V visible.

on the borders of digit primordia II, III and IV and the interdigital region by stage HH25 (Fig 13D).

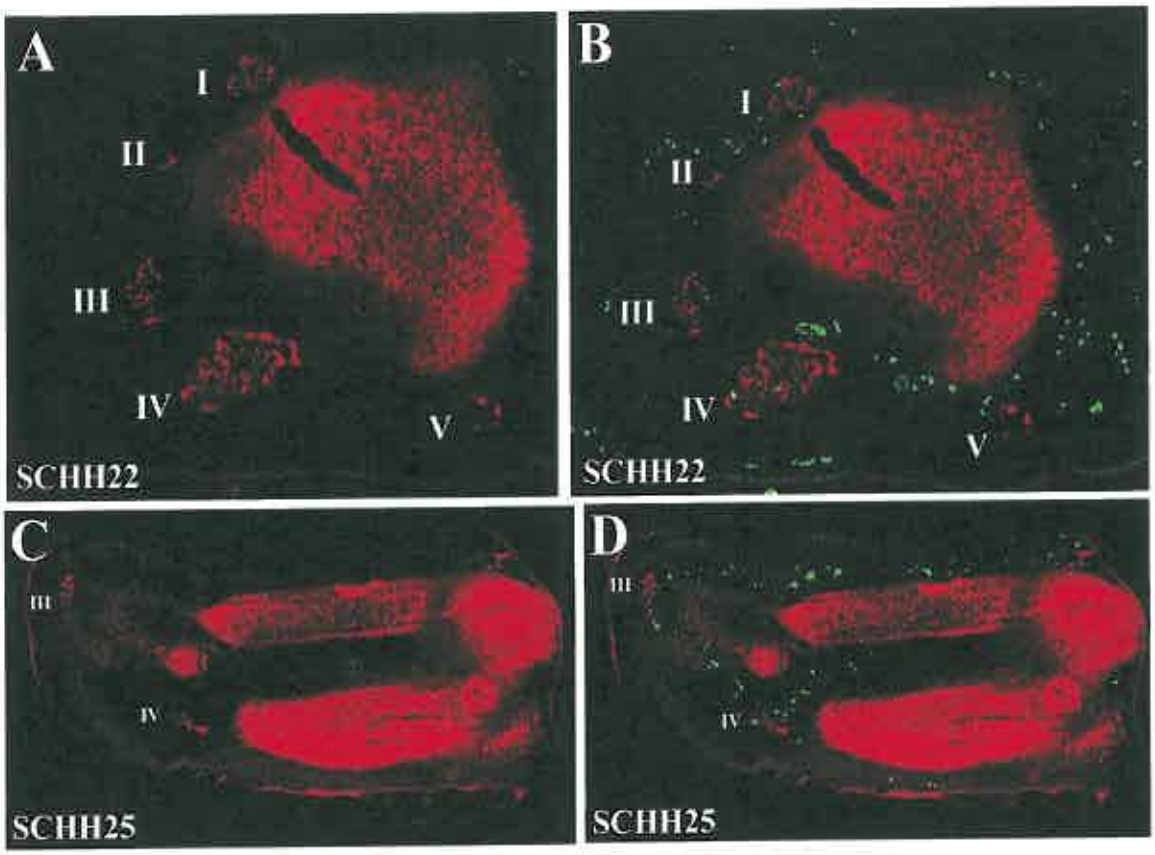

Figure 14 Sections of a *S. camelus* hind limb. A and B are hind limbs sectioned at stage SCHH22, treated with a TUNEL detection kit, anti-Sox9 and anti-mouse secondary antibody. 14A) Is a section with only the Sox9 (red) shown and 14B) is the section with both Sox9 and apoptotic nuclei (green). In both 14A and 14B, 5 digit primordia are visible, and in 14B apoptotic nuclei are visible in the interdigit regions. 14C and 14D are hind limbs sectioned at stage SCHH25. 14C) Is a section with only the Sox9 shown and 14D) is the section with both Sox9 and apoptotic nuclei . Only digits II and IV are visible in 14C and 14D while apoptotic nuclei can be seen in the interdigital regions and the region between the developing radius and ulna

3.4 TUNEL and Immunocytochemistry

A TUNEL assay and ICC was performed on sections of *S. camelus* hind limbs to assay cartilage formation and cell death in the developing limb. Figure 14A and 14B is a section through an

S. camelus hind limb at stage SCHH23. At Stage SCHH23, five cartilaginous processes can be observed marking digit primordia, as well as the cartilaginous precursor of the zeugopod. The TUNEL assay did not give conclusive results. The fluorescein, marking cell death, appeared in non-distinct areas. However, few apoptotic nuclei can be seen overlapping with digit II, IV and V primordia. By stage SCHH25 (Fig. 14C and 14D), only digit primordia III and IV can be seen, as well as the more developed zeugopod, with the radius and ulna distinguishable.

3.5 Promoter Analysis

The colony PCR yielded positive results. Bands of the correct size (3.5kb) were observed on the agarose gel run with the products of the colony PCR (fig. 15). A negative control was also performed with no templated, which yielded an empty lane (fig. 15, lane 1).

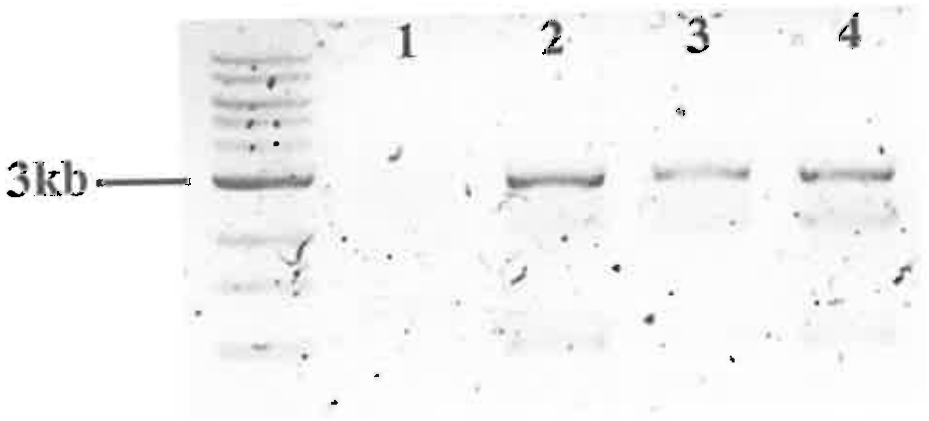

Figure 15 Agarose gel after colony PCR was performed. Lane one was a no template negative control. Lanes two, three and four were the products of successful colony PCR's. The expected product size was 3.5kb and the bands of the colony PCR products have resolved in line with the 3kb band of the molecular weight marker.

Following electroporation and incubation, live embryos were harvested. The survival rate of the embryos 48 hours after electroporation was about 25%. Expression from neither pTK-EGFP-Msx nor pCIG-RFP was observed in the limbs of the surviving embryos, however fluorescence was observed in other areas of the embryo (Fig. 16). The dead embryos were not

viewed as they develop auto-fluorescence. Some of the EGFP and RFP fluorescent markers over lapped while others were individually expressed.

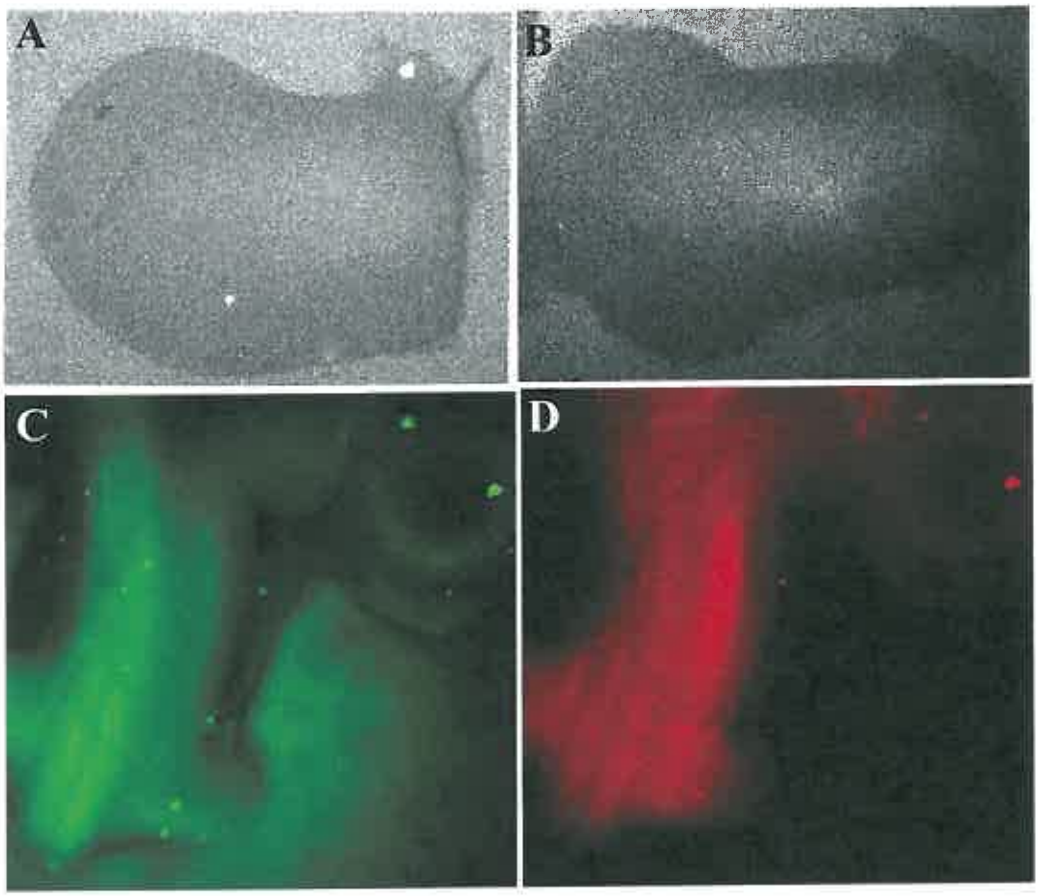

Figure 16 *G. gallus* tissue 48 hours after electroporation. Images A and B are of limbs which have been dissected off a *G. gallus* embryo at stage HH24. No fluorescence is detected. 16C) is the ventral view of the trunk region of *G. gallus* embryo at stage HH24 viewed with the EGFP filter. Non-specific fluorescence can be detected 16D) is the same embryo viewed with the RFP filter. Non-specific fluorescence is also detected with this filter.

4. Discussion

Following this study, we are able to provide evidence that programmed cell death may drive digit loss in *S. camelus*. These findings are mainly evidenced by *Msx1* and *Msx2* expression in WISH and Sox9 expression in ICC.

4.1 *Msx* expression patterns in *S. camelus* suggests its possible role in elimination digit primordia

Msx1 and *Msx2* mRNA are expressed in the interdigital regions of both *G. gallus* and *S. camelus*. Evidence suggests that these two genes have redundant functions in their roles in limb development as single homozygous mutants for either gene show insignificant limb defects, whereas the phonotypes of double homozygous mutants display severe limb defects (Lallemand *et al.*, 2005).

Expression patterns of *Msx1* and *Msx2* in *S. camelus* show the expansion of these genes into the domains of the eradicated digit primordia. In both the cases of *Msx1* and *Msx2* expression, the digit primordia of digits II, III, IV and V are visible at stage SCHH23. By SCHH25, only the primordia of digits III and IV remain, while the expression of *Msx1* and *Msx2* have expanded into the domains of digits II and V. *Msx* genes are associated with cell death as evidenced by the expression of *Msx* genes in *G. gallus* limbs in areas of cell death (Gañan *et al.*, 1998). We also observe that the expansion of *Msx2* expression into the digit primordia leads to the eradication of that primordia as well as the occurrence of TUNEL positive nuclei in these regions of expansion, as seen in the horse, camel and three-toed jerboa (Cooper *et al.*, 2014). Together these observations provide evidence that the digit primordia of digits I, II and V in the *S. camelus* hind limb may be eliminated by programmed cell death.

4.2 Loss of digit primordia in *S. camelus* could be as a result of apoptosis

The ICC and TUNEL assay showed the formation of 5 digit primordia at stage SCHH22 with possible apoptotic nuclei overlapping on digit II, IV and V primordia, the digits which are lost. The fluorescein signals, marking apoptotic nuclei, do not appear to be specific. However, the absence of fluorescein signal in the forearm precartilage and the presence the fluorescein signal in the interdigital regions indicate a degree of specificity. At a later stage, SCHH25, we see only 2 digit primordia, digits III and IV. At stage SCHH25 apoptotic nuclei can be seen in the interdigital regions, the anterior margin of the limb and the region between the tibia and fibula.

Previous studies were clearly able to associate areas of *Msx2* expression with areas of PCD indicated by TUNEL positive nuclei (Cooper *et al.*, 2014). That same clarity was not achieved in this study, however the observed loss in cartilage digit precursors from ICC supports the findings of WISH.

4.3 *Bmp* expression in *G. gallus* interdigital regions points to a role in PCD

We see in *G. gallus* limbs that *Msx* and *Bmp* genes are expressed in the same interdigital regions at the same stages. This co-expression is an indication of their possible interaction. *Bmp2* and *Bmp4* mRNA expression is seen in the interdigital regions of the developing *G. gallus* limb bud, in agreement with previously published work (Geetha-Loganathan *et al.*, 2006). WISH was not performed on *S. camelus* limbs due to a limited supply of ostrich eggs. From stage HH24 to HH25, the expansion of *Bmp2* expression can be seen moving to the digit V domain which is lost, affirming the possible contributing role of Bmp's in PCD. No *Bmp2* expression is seen in the very distal margin of the limb bud, owing to the fact that *Bmp2* is inhibited by

GREMLIN in this region, which prevents Bmp's from inhibiting *Fgf's* in the AER (M.K. Khokha *et al.*, 2003).

4.4 Expression of *Shh, Sox9* and *Fgf10* could have rules out other mechanisms of digit loss

The assessment of the expression of the additional genes, *Shh, Sox9* and *fgf10,* in *S. camelus* was intended to exclude their activity in the digit loss mechanism. Due to the above mentioned limit in the supply of ostrich eggs, WISH was not performed on *S. camelus* limbs with the probes of *Fgf10, Sox9,* and *Shh.*

Sox9 expression in *G. gallus* is as expected. By stage HH25 the digits which become ossified, digits II-V, are stained by the *Sox9* probe. The staining around digits II and III are unclear because of over staining. Being a cartilage precursor (Bi *et al.*, 1999), *Sox9* expression in *S. camelus* would have better demonstrated the loss of the digit primordia with the staining of the precartilage primordia, as opposed to the interdigital regions staining achieved with the *Msx* and *Bmp* probe staining. Additionally, the *Sox9* staining from WISH could be used to corroborate the Sox9 staining from ICC.

Shh expression in the posterior of the *G. gallus* limb bud at stage HH23 is as expected and in line with previous finding. *Shh* is secreted from the ZPA located in the posterior of the limb bud (Riddle *et al.*, 1993). Evidence has shown that digit loss in *S. camelus* takes place post patterning, well after Shh shapes the limb (de Bakker *et al.*, 2014). We have seen that altered *Shh* expression leads to digit loss in *H. quadrilineata* and that late delayed *Shh* expression in bats results in highly modified forelimbs (Hockman *et al.*, 2008; Cooper *et al.*, 2014). The expression of *Shh* was to be assessed in the *S. camelus* to more confidently preclude it from the digit loss process.

Fgf10 is essential in limb bud outgrowth, as the limb bud growth of *Fgf10*$^{-/-}$ mice is initiated, but terminated in early development (Sekine *et al.*, 1999). *Fgf10* also initiates and upregulates the expression of *Fgf8,* which upregulates *Fgf10* in a positive feedback loop. We see that *Fgf8* expression in the ossified three-toed jerboa, horse and camel is maintained in the AER above the digits which become ossified. The expression of *Fgf's* are also inhibited by Bmps (Macias *et al.*, 1996; Mustafa K Khokha *et al.*, 2003). At stage HH25 in the *G. gallus* limb bud *Fgf10* is expressed in the margins of the primordia of digits II, III and IV and not in the interdigital regions where *Bmp's* are expressed. Given the fact that *Fgfs* are inhibited by *Bmps*, the expansion of *Bmp* expression would have a concomitant reduction in *Fgf10* expression giving us further insight into PCD in *S. camelus.*

4.5 *S. camelus Msx2* promoter is able to drive expression in *G. gallus*

The intention of transfecting *G. gallus* tissue with a portion of the *S. camelus Msx2* upstream region was to gain insight into the factors that drive the expression of *Msx2* in *S. camelus.* An upstream region of *Msx2* has been shown to bind *Bmp4,* presumably to initiate PCD. In the later stages of limb development when *Fgf* signalling from the AER begins to attenuate, so does the expression of *Gremlin,* the *Bmp* inhibitor. Without Gremlin inhibition, Bmp4 is able to bind the *Msx2* promoter and drive ICD. How PCD is restricted to the interdigital regions is still unknown. It could be an alteration in the *S. camelus Msx2* promoter, which changes how it interacts with Bmp4 which could yield the unique hind limb morphology of *S. camelus.*

Expression of neither the EGFP from pTK-EGFP-Msx nor RFP from pCIG-RFP was achieved in the developing limb buds of *G. gallus*. Expression was observed in other embryonic tissue, mainly in the trunk region. pCIG-RFP contains the CAG promoter, which is able to drive expression in *G. gallus.* The low levels of RFP expression indicates low plasmid uptake and

expression, which could result from suboptimal electroporation conditions. The tissue into which the plasmid was injected was solid, which is not ideal for the retention of the plasmid mixture, resulting in much of the plasmid being lost outside of the tissue, leaving little for electroporation.

Expression of EGFP was also observed in the trunk region. This indicated that the 3.5kb region upstream of *S. camelus* is able to drive expression in *G. gallus*. These results do not give us any information about the factors that contribute to this expression, such as the transcription factors involved. What we can infer is that it is able to drive expression and that the expression is not limb specific.

4.6 Conclusion

It has been shown that *Msx1,* and *Msx2* expression domains expand into the domains of the eradicated digits, and the possible presence of apoptotic nuclei with in those digit primordia. Preliminary evidence has therefore been presented herein to suggest that post patterning programmed cell death involving *Msx1* and *Msx2* pathways drives digit loss in the hind limbs of *S. camelus*.

It was also noted that a 3.5kb region upstream of the *S. camelus Msx2* gene is able to drive EGFP expression in *G. gallus,* however this information, while novel and potentially significant, did not contribute to the elucidating the mechanisms of digit loss in *S. camelus*.

There are many genes and many interlinking pathways involved in limb development, as such, further investigation into the subject would have to be made, investigating the roles of other genes in the process for a decisive conclusion to be made.

4.7 Further work

More investigation is required to confirm the mechanism of digit loss in *S. camelus*. The expression patterns of *Sox9, Shh, Fgf10* and *Fgf8* in the *S. camelus* limb should be investigated to exclude any post patterning developmental mechanisms which may shape the limb. Better analysis of the occurrence of apoptosis in the developing limb bud should be obtained to get a clearer idea of cell death during development, as well as knock out experiments involving *Msx2* and *Bmp4*, and possible their homologs. A more in depth investigation of the *Msx2* promoter and its interaction with Bmp4 should also be done.

5.1 Appendix A

Solutions used in *in situ* hybridisation

Phosphate buffered saline	
$Na_2HPO4 \cdot 7H_2O$	43mM
NaCl	1.4M
KH_2PO_4	14mM
KCl	27mM
Tween-20	0.1%
H_2O	To required volume

Hybridisation mix	
Formamide	5%
20X SCC	2.5%
H_2O_2	28%
Heparin	100µg
10% CHAPS	0.5%
Tween-20	0.2%
tRNA (If required)	200µ/ml
H_2O (DEPC)	To required volume

20X SCC pH5.0	
NaCl	3M
Monosodium citrate	0.4M
H_2O (DEPC)	To required volume

5X MABT pH7.5	
Maleic acid	0.5M
Tris-base (to pH 7.5)	0.8M – 1.2M
NaCl	0.75M
Tween-20	0.1%
H_20	To required volume

NTMT pH9.5	
NaCl	100mM
Tris-base	100mM
$MgCl_2$	50mM
Tween-20	0.1%
H_2O	To required volume

5.2 Appendix B

Sources of figure 5B images

Nile crocodile – by Jocelyn Ouellet @ http://www.jnomade.org/en/photoblog/trip2/kenya/kitale/

Ostrich - http://web.stanford.edu/~siegelr/RSA/gardenroute/IMG_0676%20ostrich%20foot.jpg

Emu - https://iamsafari.com/2015/02/15/yalabidi-walking-with-dinosaurs/

Barbary dove - http://pet-doves.com/petdoves/dove_selection.htm

Zebra finch - https://www.etsy.com/listing/228807249/tiny-finch-feet-real-matched-set-dry

Chicken - http://www.sendirimu.xyz/live-chicken-feet/

Zebra - http://www.ponyville.se/hovar_en.html

Sumatran rhino - http://www.arkive.org/black-rhinoceros/diceros-bicornis/image-G112062.html

Baird's tapir - http://www.alamy.com/stock-photo-the-hind-feet-of-a-bairds-tapir-tapirus-bairdii-75530114.html

Bactrian camel - https://za.pinterest.com/pin/406731410077898624/

Hippopotamus - https://za.pinterest.com/pin/468937379929757939/

Wild boar - https://za.pinterest.com/birdydrew/warthogs-boars/

Chacoan peccary - http://www.arkive.org/chacoan-peccary/catagonus-wagneri/

Sheep - http://anatomyofthefoot.com/anatomy-of-sheep-foot.html

Water buffalo - https://www.flickr.com/photos/75164718@N08/6756079809

Cattle - http://www.fmdinfo.org/images.aspx

Red deer - https://za.pinterest.com/pin/207869339026426092/

Water deer - https://za.pinterest.com/pin/324962929336740345/

Reindeer - https://www.dreamstime.com/stock-photos-plane-towing-glider-airplane-aircraft-cloudscape-background-image31476323

Moose - https://hoofcare.blogspot.co.za/2011/10/laminitis-in-moose-vermonts-pete-moose.html

6. References

Ahn, D. G., Kourakis, M. J., Rohde, L. A., Silver, L. M. and Ho, R. K. (2002) 'T-box gene tbx5 is essential for formation of the pectoral limb bud.', *Nature*, 417(6890), pp. 754–758.

Ahn, K., Mishina, Y., Hanks, M. C., Behringer, R. R. and Iii, E. B. C. (2001) 'BMPR-IA signaling is required for the formation of the apical ectodermal ridge and dorsal-ventral patterning of the limb', 128(22), pp. 4449–4461.

de Bakker, M. A. J., Fowler, D. A., den Oude, K., Dondorp, E. M., Navas, M. C. G., Horbanczuk, J. O., Sire, J. Y., Szczerbinska, D. and Richardson, M. K. (2014) 'Digit loss in archosaur evolution and the interplay between selection and constraints', *Nature*, 500, pp. 445–450. doi: 10.1038/nature12336.

de Bakker, M. a G., Fowler, D. a, den Oude, K., Dondorp, E. M., Navas, M. C. G., Horbanczuk, J. O., Sire, J.-Y., Szczerbińska, D. and Richardson, M. K. (2013) 'Digit loss in archosaur evolution and the interplay between selection and constraints.', *Nature*, 500(7463), pp. 445–8. doi: 10.1038/nature12336.

Bénazet, J. D. and Zeller, R. (2009) 'Vertebrate limb development: moving from classical morphogen gradients to an integrated 4-dimensional patterning system.', *Cold Spring Harbor perspectives in biology*, 1(4), p. p.a001339.

Bendall, A. and Abate-Shen, C. (2000) 'Roles for Msx and Dlx homeoproteins in vertebrate development.', *Gene*, 247, p. 17–31.

Bensoussan-Trigano, V., Lallemand, Y., Saint Cloment, C. and Robert, B. (2011) 'Msx1 and Msx2 in limb mesenchyme modulate digit number and identity', *Developmental Dynamics*, 240(5), pp. 1190–1202. doi: 10.1002/dvdy.22619.

Van den berg, C. and Rayner, J. M. V. (1995) 'The moment of inertia of bird wings and the inertial power requirement for flapping flight.', *J. Exp. Biol.*, 198(8), pp. 1655–1664.

Bi, W., Deng, J. M., Zhang, Z., Behringer, R. R. and de Crombrugghe, B. (1999) 'Sox9 is required for cartilage formation.', *Nature genetics*, 22(1), pp. 85–89.

Brand, Z., Cloete, S. W. P., Malecki, I. A. and Brown, C. R. (2012) 'Heritability of embryonic mortalities in ostrich eggs and factors affecting hatching failure of fertile eggs during artificial incubation.', *Animal production science*, 52(9), pp. 806–812.

Brand, Z., Cloete, S. W. P., Malecki, I. A. and Brown, C. R. (2017) 'Ostrich (Struthio camelus) embryonic development from 7 to 42 days of incubation.', *British poultry science*, 58(2), pp. 139–143.

Briscoe, J., Chen, Y., Jessell, T. M. and Struhl, G. (2001) 'A hedgehog-insensitive form of Patched provides evidence for direct long-range morphogen activity of Sonic hedgehog in the neural tube', *Molecular Cell*, 7(6), pp. 1279–1291. doi: 10.1016/S1097-2765(01)00271-4.

Brown, C. R. and Prior, S. A. (1999) 'Development of body temperature regulation in ostrich chicks.', *British poultry science*, 40(4), pp. 529–535.

Brugger, S. M., Merrill, A. E., Torres-Vazquez, J., Wu, N., Ting, M.-C., Cho, J. Y.-M.,

Dobias, S. L., Yi, S. E., Lyons, K., Bell, J. R., Arora, K., Warrior, R. and Maxson, R. (2004) 'A phylogenetically conserved cis-regulatory module in the Msx2 promoter is sufficient for BMP-dependent transcription in murine and Drosophila embryos.', *Development (Cambridge, England)*, 131(20), pp. 5153–5165. doi: 10.1242/dev.01390.

Capdevila, J., Tsukui, T., Esteban, C. R., Zappavigna, V. and Belmonte, J. C. I. (1999) 'Control of vertebrate limb outgrowth by the proximal factor Meis2 and distal antagonism of BMPs by Gremlin.', *Molecular cell*, 4(5), pp. 839–849.

Charité, J., McFadden, D. G. and Olson, E. N. (2000) 'The bHLH transcription factor dHAND controls Sonic hedgehog expression and establishment of the zone of polarizing activity during limb development.', *Development (Cambridge, England)*, 127(11), pp. 2461–2470.

Chautan, M., Chazal, G., Cecconi, F., Gruss, P. and Golstein, P. (1999) 'Interdigital cell death can occur through a necrotic and caspase-independent pathway.', *Current biology*, 9(17), pp. 967-S1.

Chen, Y., Bei, M., Woo, I., Satokata, I. and Maas, R. (1996) 'Msx1 controls inductive signaling in mammalian tooth morphogenesis.', *Development*, 122(10), pp. 3035–3044.

Chen, Y. and Struhl, G. (1996) 'Dual roles for patched in sequestering and transducing Hedgehog.', *Cell*, 87(3), pp. 553–563.

Clarke, P. G. (1990) 'Developmental cell death: morphological diversity and multiple mechanisms.', *Anatomy and embryology*, 181(3), pp. 195–213.

Cohn, M. J., Izpisúa-Belmonte, J. C., Abud, H., Heath, J. K. and Tickle, C. (1995) 'Fibroblast growth factors induce additional limb development from the flank of chick embryos.', *Cell*, 80(5), pp. 739–746.

Cooper, K. L., Sears, K. E., Uygur, A., Maier, J., Baczkowski, K.-S., Brosnahan, M., Antczak, D., Skidmore, J. a and Tabin, C. J. (2014) 'Patterning and post-patterning modes of evolutionary digit loss in mammals.', *Nature*. Nature Publishing Group, 511(7507), pp. 41–5. doi: 10.1038/nature13496.

Crossley, P. H., Minowada, G., MacArthur, C. A. and Martin, G. R. (1996) 'Roles for FGF8 in the induction, initiation, and maintenance of chick limb development.', *Cell*, 84(1), pp. 127–136.

Davidson, D. (1995) 'The function and evolution of Msx genes: pointers and paradoxes.', *Trends Genet*, 11(10), pp. 405–411.

Davis, C. A. and Joyner, A. L. (1988) 'Expression patterns of the homeo box-containing genes En-1 and En-2 and the proto-oncogene int-1 diverge during mouse development.', *Genes & Development*, 2(12b), pp. 1736–1744.

Dealy, C. N., Roth, A., Ferrari, D., Brown, A. M. and Kosher, R. A. (1993) 'Wnt-5a and Wnt-7a are expressed in the developing chick limb bud in a manner suggesting roles in pattern formation along the proximodistal and dorsoventral axes.', *Mechanisms of development*, 43(2), p. 175–186.

Dolle, P., Dierich, a., LeMeur, M., Schimmang, T., Schuhbaur, B., Chambon, P. and Duboule, D. (1993) 'Disruption of the Hoxd-13 gene induces localized heterochrony leading

to mice with neotenic limbs', *Cell*, 75(3), pp. 431–441. doi: 10.1016/0092-8674(93)90378-4.

Drossopoulou, G., Lewis, K. E., Sanz-Ezquerro, J. J., Nikbakht, N., McMahon, A. P., Hofmann, C. and Tickle, C. (2000) 'A model for anteroposterior patterning of the vertebrate limb based on sequential long-and short-range Shh signalling and Bmp signalling.', *Development*, 127(7), pp. 1337–1348.

Erickson, C. J. (1994) 'Tap-scanning and extractive foraging in aye-ayes, Daubentonia madagascariensis.', *Folia Primatologica*, 62(1–3), pp. 125–135.

Fallon, J. F. and Crosby, G. M. (1977) 'Polarizing zone activity in limb buds of amniotes.', *Vertebrate limb and somite morphogenesis*, pp. 55–69.

Favier, B., Rijli, F. M., Fromental-Ramain, C., Fraulob, V., Chambon, P. and Dollé, P. (1996) 'Functional cooperation between the non-paralogous genes Hoxa-10 and Hoxd-11 in the developing forelimb and axial skeleton.', *Development (Cambridge, England)*, 122(2), pp. 449–460.

Ferrari, D., Lichtler, a C., Pan, Z. Z., Dealy, C. N., Upholt, W. B. and Kosher, R. a (1998) 'Ectopic Expression ofMsx-2in Posterior Limb Bud Mesoderm Impairs Limb Morphogenesis While InducingBMP-4Expression, Inhibiting Cell Proliferation, and Promoting Apoptosis.', *Developmental biology*, 197(1), pp. 12–24. doi: 10.1006/dbio.1998.8880.

Fromental-Ramain, C., Warot, X., Messadecq, N., LeMeur, M., Dollé, P. and Chambon, P. (1996) 'Hoxa-13 and Hoxd-13 play a crucial role in the patterning of the limb autopod.', *Development (Cambridge, England)*, 122(10), pp. 2997–3011.

Gañan, Y., Macias, D., Basco, R. D., Merino, R. and Hurle, J. M. (1998) 'Morphological diversity of the avian foot is related with the pattern of msx gene expression in the developing autopod.', *Developmental biology*, 196(1), pp. 33–41. doi: 10.1006/dbio.1997.8843.

Gañan, Y., Macias, D., Duterque-Coquillaud, M., Ros, M. a and Hurle, J. M. (1996) 'Role of TGF beta s and BMPs as signals controlling the position of the digits and the areas of interdigital cell death in the developing chick limb autopod.', *Development (Cambridge, England)*, 122(8), pp. 2349–2357.

Geetha-Loganathan, P., Nimmagadda, S., Huang, R., Scaal, M. and Christ, B. (2006) 'Expression pattern of BMPs during chick limb development.', *Anatomy and embryology*, 211(1), pp. 87–93.

Graham, A., Francis-West, P., Brickell, P. and Lumsden, A. (1994) 'The signalling molecule BMP4 mediates apoptosis in the rhombencephalic neural crest.', *Nature*, 372(6507), pp. 684–686.

Groves, C. P. (2001) 'Primate Taxonomy.', *Washington, Smithsonian Institution Press.*

Hamburger, V. and Hamilton., H. L. (1951) 'A Series of Normal Stages in the Development of the Chick Embryo', *J Morphol.*, 81(1), pp. 49–92. doi: 10.1002/aja.1001950404.

Hengartner, M. O. (2000) 'The biochemistry of apoptosis.', *Nature*, 407(6805), p. 770.

Hernández-Martínez, R. and Covarrubias, L. (2011) 'Interdigital cell death function and regulation: new insights on an old programmed cell death model.', *Development, growth & differentiation*, 53(2), pp. 245–258. doi: 10.1111/j.1440-169X.2010.01246.x.

Hockman, H., Cretekosb, C. J., Masonc, M. K., Behringerd, R. R., Jacobsc, D. S. and Illinga, N. (2008) 'A second wave of sonic hedgehog expression during the development of the bat limb', *PNAS*, 105(44), pp. 16982–16987.

Jacobson, M., Weil, M. and Raff, M. (1997) 'Programmed cell death in animal development.', *Cell*, 88(1), pp. 347–354. doi: 10.1016/S0092-8674(00)81873-5.

Jouffroy, F. K., Godinot, M., and Nakano, Y. and 1993. (1993) 'Biometrical characteristics of primate hands.', in *In Hands of primates*. Springer Vienna, pp. 133–171.

Kawakami, Y., Capdevila, J., Buscher, D., Itoh, T., Rodriguez Esteban, C. and IzpisuaBelmonte, J. (2001) 'WNT signals control FGF-dependent limb initiation and AER induction in the chick embryo.', *Cell*, 104(6), pp. 891–900.

Khokha, M. K., Hsu, D., Brunet, L. J., Dionne, M. S. and Harland, R. M. (2003) 'Gremlin is the BMP antagonist required for maintenance of Shh and Fgf signals during limb patterning.', *Nat Genet 34: 303–307.*

Khokha, M. K., Hsu, D., Brunet, L. J., Dionne, M. S. and Harland, R. M. (2003) 'Gremlin is the BMP antagonist required for maintenance of Shh and Fgf signals during limb patterning.', *Nature genetics*, 34(3), pp. 303–7. doi: 10.1038/ng1178.

Kingsley, D. M. (1994) 'The TGF-beta superfamily: new members, new receptors, and new genetic tests of function in different organisms.', *Genes Dev*, 8(2), pp. 133–146.

Kmita, M., Tarchini, B., Zakany, J., Logan, M., Tabin, C. J. and Duboule, D. (2005) 'Early developmental arrest of mammalian limbs lacking HoxA/HoxD gene function', *Nature*, 435(7045), pp. 1113–1116. doi: 10.1038/nature03648.

Lallemand, Y., Nicola, M.-A., Ramos, C., Bach, A., Cloment, C. Saint and Robert, B. (2005) 'Analysis of Msx1; Msx2 double mutants reveals multiple roles for Msx genes in limb development.', *Development (Cambridge, England)*, 132(13), pp. 3003–3014. doi: 10.1242/dev.01877.

Lande, R. (1978) 'Evolutionary mechanisms of limb loss in tetrapods.', *Evolution*, 32, pp. 73–92.

Laufer, E., Dahn, R., Orozco, O. E., Yeo, C. Y., Pisenti, J., Henrique, D., Abbot, U. K., Fallon, J. F. and Tabin, C. (1997) 'expression of Radical fringe in limb-bud ectoderm regulates apical ectodermal fidge formation', *Nature*, 386(6623), pp. 366–373.

Litingtung, Y., Dahn, R. D., Li, Y., Fallon, J. F. and Chiang, C. (2002) 'Shh and Gli3 are dispensable for limb skeleton formation but regulate digit number and identity.', *Nature*, 418(6901), pp. 979–983. doi: 10.1038/nature01033.

Logan, M. (2003) 'Finger or toe: the molecular basis of limb identity.', *Development*, 130(26), pp. 6401–6410.

Lopez-Rios, J., Duchesne, A., Speziale, D., Andrey, G., Peterson, K. A., Germann, P., Ünal, E., Liu, J., Floriot, S., Barbey, S., Gallard, Y., Müller-Gerbl, M., Courtney, A. D., Klopp, C., Rodriguez, S., Ivanek, R., Beisel, C., Wicking, C., Iber, D., Robert, B., McMahon, A. P., Duboule, D. and Zeller, R. (2014) 'Attenuated sensing of SHH by Ptch1 underlies evolution of bovine limbs', *Nature*, pp. 1–16. doi: 10.1038/nature13289.

Lorda-Diez, C. I., Garcia-Riart, B., Montero, J. A., Rodriguez-León, J., Garcia-Porrero, J. A. and Hurle, J. M. (2015) 'Apoptosis during embryonic tissue remodeling is accompanied by cell senescence.', *Aging (Albany NY)*, 7(11), p. 974.

Maatouk, D. M., Choi, K. S., Bouldin, C. M. and Harfe, B. D. (2009) 'In the limb AER Bmp2 and Bmp4 are required for dorsal–ventral patterning and interdigital cell death but not limb outgrowth.', *Developmental biology*, 327(2), pp. 516–523.

Macias, D., Gañan, Y., Ros, M. A. and Hurle, J. M. (1996) 'In vivo inhibition of programmed cell death by local administration of FGF-2 and FGF-4 in the interdigital areas of the embryonic chick leg bud.', *Anatomy and embryology*, 193(6), pp. 533–541.

Macias, D., Ros, M. A., Sampath, T. K., Piedra, M. E. and Hurle, J. M. (1997) 'Role of BMP-2 and OP-1 (BMP-7) in programmed cell death and skeletogeneis during chick limb development', *Development*, 124(6), pp. 1109–1117.

Marazzi, G., Wang, Y. and Sassoon, D. (1997) 'Msx2 is a transcriptional regulator in the BMP4-mediated programmed cell death pathway.', *Developmental biology*, 186(2), pp. 127–138. doi: 10.1006/dbio.1997.8576.

Marom, B., Heining, E., Knaus, P. and Henis, Y. I. (2011) 'Formation of stable homomeric and transient heteromeric bone morphogenetic protein (BMP) receptor complexes regulates Smad protein signaling.', *Journal of Biological Chemistry*, 286(22), pp. 19287–19296.

Martin, G. R. (1998) 'The roles of FGFs in the early development of vertebrate limbs.', *Genes & Development*, 12(11), pp. 1571–1586.

Martin, R. E., Pine, R. H. and DeBlase, A. F. (2001) *A Manual of Mammalogy, with keys to familes of the world*. 3rd edn. Wavelend Press.

Massagué, J., Seoane, J. and Wotton, D. (2005) 'Smad transcription factors.', *Genes & development*, 19(23), pp. 2783–2810.

Merino, R., Rodriguez-Leon, J., Macias, D., Gañan, Y., Economides, a N. and Hurle, J. M. (1999) 'The BMP antagonist Gremlin regulates outgrowth, chondrogenesis and programmed cell death in the developing limb.', *Development*, 126(23), pp. 5515–5522.

Milliken, G. W., Ward, J. P. and Erickson, C. J. (1991) 'Independent digit control in foraging by the aye-aye (Daubentonia madagascariensis).', *Folia Primatologica*, 56(4), pp. 219–224.

Montero, J. A., Sanchez-Fernandez, C., Lorda-Diez, C. I., Garcia-Porrero, J. A. and Hurle, J. M. (2016) 'DNA damage precedes apoptosis during the regression of the interdigital tissue in vertebrate embryos.', *Scientific reports*, 6.

Moon, A. M. and Capecchi, M. R. (2000) 'Fgf8 is required for outgrowth and patterning of the limbs.', *Nat Genet*, 26(4), pp. 455–45.

Mori, C., Nakamura, N., Kimura, S., Irie, H., Takigawa, T. and Shiota, K. (1995) 'Programmed cell death in the interdigital tissue of the fetal mouse limb is apoptosis with DNA fragmentation.', *The Anatomical Record, 242(1), Pp.103-110.*, 242(1), pp. 103–110.

Niswander, L., Tickle, C., , Vogel, A., Booth, I. and Martin, G. R. (1993) 'FGF-4 replaces the apical ectodermal ridge and directs outgrowth and patterning of the limb.', *Cell*, 75(3), pp. 579–587.

Okabe, M., Ikawa, M., Kominami, K., Nakanishi, T. and Nishimune, Y. (1997) '"Green mice"as a source of ubiquitous green cells.', *FEBS letters*, 407(3), pp. 313–319.

Pizette, S., Abate-shen, C. and Niswander, L. (2001) 'BMP controls proximodistal outgrowth , via induction of the apical ectodermal ridge , and dorsoventral patterning in the vertebrate limb', *Development*, 128(22), pp. 4463–4474.

Pizette, S. and Niswander, L. (1999) 'BMPs negatively regulate structure and function of the limb apical ectodermal ridge.', *Development, 126(5), pp.883-894.*, 126(5), pp. 883–894.

Riddle, R. D., Ensini, M., Nelson, C., Tsuchida, T., Jessell, T. M. and Tabin, C. (1995) 'Induction of the LIM homeobox gene Lmx1 by WNT6a establishes dorsoventral pattern in the vertebrate limb.', *Cell*, 83(4), p. 631–640.

Riddle, R. D., Johnson, R. L., Laufer, E. and Tabin, C. (1993) 'Sonic hedgehog mediates the polarizing activity of the ZPA', *Cell*, 75(7), pp. 1401–1416. doi: 10.1016/0092-8674(93)90626-2.

Rodriguez-Esteban, C., Tsukui, T., Yonei, S., Magallon, J., Tamura, K. and Belmonte, J. C. I. (1999) 'The T-box genes Tbx4 and Tbx5 regulate limb outgrowth and identity.', *Nature*, 398(6730), pp. 814–818.

Rowe, D. A. and Fallon, J. F. (1982) 'The proximodistal determination of skeletal parts in the developing chick leg.', *J. Embryol. Exp. Morphol.*, 68(1), pp. 1–7.

Saunders, J. W. (1948) 'The proximo-distal sequence of the origin of the parts of the chick wing and the role of the ectoderm.', *J. Exp. Zool.*, 108(3), pp. 363–403.

Van Schalkwyk, S. J., Brand, Z., Cloete, S. W. P. and Brown, C. R. (1999) 'Effects of time of eggs collection and pre-incubation treatment on blastoderm development and embryonic mortality in ostrich embryos.', *South African Journal of Animal Science, 29(3).*, 29(3).

Schaller, N. U., D'Août, K., Villa, R., Herkner, B. and Aerts, P. (2011) 'Toe function and dynamic pressure distribution in ostrich locomotion.', *The Journal of experimental biology*, 214(7), pp. 1123–1130. doi: 10.1242/jeb.043596.

Sears, K. E., Bormet, A. K., Rockwell, A., Powers, L. E., Noelle Cooper, L. and Wheeler, M. B. (2011) 'Developmental basis of mammalian digit reduction: a case study in pigs.', *Evolution & development*, 13(6), pp. 533–541.

Sekine, K., Ohuchi, H., Fujiwara, M., Yamasaki, M., Yoshizawa, T., Sato, T., Yagishita, N., Matsui, D., Koga, Y., Itoh, N. and Kato, S. (1999) 'Fgf10 is essential for limb and lung formation', *Nature genetics*, 21(1), pp. 138–141.

Shapiro, M. D., Hanken, J. and Rosenthal, N. (2003) 'Developmental basis of evolutionary digit loss in the Australian lizard Hemiergis.', *Journal of experimental zoology. Part B, Molecular and developmental evolution*, 297(1), pp. 48–56. doi: 10.1002/jez.b.00019.

Sheth, R., Bastida, M. F. and Ros, M. (2007) 'Hoxd and Gli3 interactions modulate digit number in the amniote limb', *Developmental Biology*, 310(2), pp. 430–441. doi: 10.1016/j.ydbio.2007.07.023.

Starck, J. M. and Ricklefs, R. E. eds. (1998) *Avian growth and development: evolution within the altricial-precocial spectrum (No. 8)*. Oxford University Press on Demand.

Summerbell, D. (1974) 'A quantitative analysis of the effect of excision of the AER from the chick limb bud.', *J. Embryol. Exp. Morphol.*, 32(3), pp. 651–660.

Sun, X., Lewandoski, M., Meyers, E. N., Liu, Y., Jr, R. E. M. and Martin, G. R. (2000) 'Conditional inactivation of Fgf4 reveals complexity of signalling during limb bud development', *Nature genetics*, 25(1), pp. 83–86.

Sun, X., Mariani, F. V and Martin, G. R. (2002) 'Functions of FGF signalling from the apical ectodermal ridge in limb development.', *Nature*, 418(6897), pp. 501–508. doi: 10.1038/nature00902.

Tarchini, B., Duboule, D. and Kmita, M. (2006) 'Regulatory constraints in the evolution of the tetrapod limb anterior–posterior polarity.', *Nature*, 443(7114), pp. 985–988.

Taylor, G. K., Nudds, R. L. and Thomas, A. L. (2003) 'Flying and swimming animals cruise at a Strouhal number tuned for high power efficiency.', *Nature*, 425(6959), pp. 707–711.

Tickle, C. (2006) 'Making digit patterns in the vertebrate limb', *Nature Reviews Molecular Cell Biology*, 7(1), pp. 45–53. doi: 10.1038/nrm1830.

Tickle, C., Summerbell, D. and Wolpert, L. (1975) 'Positional signalling and specification of digits in chick limb morphogenesis.', *Nature*, 254(5497), pp. 199–202.

Varjosalo, M. and Taipale, J. (2007) 'Hedgehog signaling', *Journal of Cell Science*, 1(120), pp. 3–6. doi: 10.1242/jcs.03309.

Vogel, A., Rodriguez, C., Warnken, W. and Izpisua Belmonte, J. C. (1995) 'Dorsal cell fate specified by chick Lmx1 during vertebrate limb development.', *Nature*, 378(6558), pp. 716–720.

Vogel, a, Rodriguez, C. and Izpisúa-Belmonte, J. C. (1996) 'Involvement of FGF-8 in initiation, outgrowth and patterning of the vertebrate limb.', *Development*, 122(6), pp. 1737–1750. doi: 10.1016/0168-9525(96)81475-2.

Wang, B., Fallon, J. F. and Beachy, P. A. (2000) 'Hedgehog-regulated processing of Gli3 produces an anterior/posterior repressor gradient in the developing vertebrate limb.', *Cell*, 100(4), pp. 423–434.

Wang, C. L., Omi, M., Ferrari, D., Cheng, H., Lizarraga, G., Chin, H., Upholt, W. B., Dealy, C. N. and Kosher, R. A. (2004) 'Function of BMPs in the apical ectoderm of the developing mouse limb', *Developmental Biology*, 269(1), pp. 109–122. doi: 10.1016/j.ydbio.2004.01.016.

Te Welscher, P., Fernandez-Teran, M., Ros, M. A. and Zeller, R. (2002) 'Mutual genetic antagonism involving GLI3 and dHAND prepatterns the vertebrate limb bud mesenchyme prior to SHH signaling', *Genes and Development*, 16(4), pp. 421–426. doi: 10.1101/gad.219202.

te Welscher, P., Fernandez-Teran, M., Ros, M. A. and Zeller, R. (2002) 'Mutual genetic antagonism involving GLI3 and dHAND prepatterns the vertebrate limb bud mesenchyme prior to SHH signaling.', *Genes & development*, 16(4), pp. 421–426.

Wolpert, L. (1969) 'Positional information and the spatial pattern of cellular differentiation..', *J. Theoret. Biol.*, 25(1), pp. 1–47.

Yokouchi, Y., Sakiyama, J., Kameda, T., Iba, H., Suzuki, A., Ueno, N. and Kuroiwa, A. (1996) 'BMP-2/-4 mediate programmed cell death in chicken limb buds.', *Development*, 122(12), pp. 3725–3734.

Zakany, J., Zacchetti, G. and Duboule, D. (2007) 'Interactions between HOXD and Gli3 genes control the limb apical ectodermal ridge via Fgf10. .', *Developmental biology*, 306(2), pp. 883–893.

Zou, H. and Niswander, L. (1995) 'Requirements for BMP Signalling in Interdigital Apoptosis and Scale Formation', *Science*, 272(6916), pp. 738–741.

Zúñiga, A., Haramis, A. P. G., McMahon, A. P. and Zeller, R. (1999) 'Signal relay by BMP antagonism controls the SHH/FGF4 feedback loop in vertebrate limb buds.', *Nature*, 401(6753), pp. 598–602.

Zuzarte-Luis, V., Berciano, M. T., Lafarga, M. and Hurle, J. M. (2006) 'Caspase redundancy and release of mitochondrial apoptotic factors characterize interdigital apoptosis.', *Apoptosis, 11(5), pp.701-715.*, 11(5), pp. 701–715.

Zuzarte-Luis, V., Montero, J. A., Kawakami, Y., Izpisua-Belmonte, J. C. and Hurle, J. M. (2007) 'Lysosomal cathepsins in embryonic programmed cell death.', *Developmental biology*, 301(1), pp. 201–217.